Notch missense mutations in *Drosophila* reveal functions of specific EGF-like repeats in Notch folding, trafficking, and signaling

ショウジョウバエ Notch 遺伝子のミスセンス突然変異を用いた EGF-様リピートの Notch 折りたたみ、輸送、シグナルにおける特異的機能の研究

A thesis

Submitted to the

Department of Biological Sciences, Graduate School of Science

Osaka University

In the fulfillment of

The requirements for the degree of Doctor of Philosophy

By

Hilman Nurmahdi

24D19891

Supervisor : Dr. Kenji Matsuno

Committee member : Dr. Naotada Ishihara

Committee member : Dr. Hiroki Oda

Committee member : Dr. Motoo Kitagawa

Table of contents

Notch missense mutations in *Drosophila* reveal functions of specific EGF-like repeats in Notch folding, trafficking, and signaling

ショウジョウバエ Notch 遺伝子のミスセンス突然変異を用いた EGF-様リピートの Notch 折りたたみ、輸送、シグナルにおける特異的機能の研究

Hilman Nurmahdi

Summary

Notch signaling plays various roles in regulating a wide range of cell-fate specifications through direct cell-cell interactions. The Notch signaling pathway is evolutionarily conserved, and aberrant Notch signaling causes various diseases in human. Currently, major processes of Notch signal transduction are well understood. Starting from when Notch ligands binds to Notch receptor, the intracellular domain of Notch is released from the plasma membrane by a proteolytic cleavage at its transmembrane domain and translocated into the nucleus where it forms a complex with transcription factors and induces the transcription of target genes. However, complex regulatory processes lie behind and are involved in the precise regulation of Notch signaling. Especially, the extracellular domain of Notch is known to play multiple roles. The Notch extracellular

domain consists of 36 Epidermal growth factor (EGF)-like repeats that play specific roles in the functions of *Notch*. Among them, EGF-like repeats 11-12 have been known to serve as the binding site for the Notch ligands, and the EGF-like repeats 24-29 are known as Abruptex domain that negatively regulates *Notch* activity. However, specific functions of each of the 36 EGF-like repeats remain unclear.

In this study, I attempted to reveal the specificities of each EGF-like repeat and cluster of them in the activity and folding of Notch. These issues were addressed by using 18 *Notch* mutant alleles carrying missense mutations that introduce single amino acid substitution in different EGF-like repeats, as well as a *Notch* mutant allele causing an amino acid substitution in the transmembrane domain of Notch. These *Notch* alleles were isolated based on loss of bristle phenotypes that suggest the loss-of-function of *Notch* in the processes of asymmetric cell division occurred during the bristle formation. It is known that Notch signaling has functions in three categories of biological processes; asymmetric cell division, lateral inhibition, and inductive signaling. Therefore, to observe the potential specificities of the defects associated with these various *Notch* mutations, I checked the phenotypes of the embryonic central nervous system and the boundary cells of the embryonic hindgut, which imply potential defects in lateral inhibition and inductive signaling, respectively. I found that only 10 out of 19 *Notch* mutants showed defects in

lateral inhibition and inductive signaling, demonstrating that these *Notch* mutants show the depletion of Notch signaling in a context-dependent manner. However, defects in lateral inhibition and inductive signaling were observed concomitantly in all cases, suggesting that the EGF-like repeats mutated in these alleles may have similar functions between these two categories of Notch signaling. From these analyses, I also found that the EGF-like repeats sensitive to the perturbation induced by amino acid substitutions appeared to cluster in a regions encompassing EGF-like repeats 8-10. Interestingly, the EGF-like repeats 8-10 include the EGF-like repeat 8 that was previously identified as a region that controls the preference of ligands binding to Notch. Additionally, I found that the EGF-like repeat 25 is also sensitive to the amino acid substitution. The EGF-like repeat 25 locates in the Abruptex domain that is known to negatively regulate *Notch* activity based on genetic analyses. Taking together, I revealed that the sensitive regions of the EGF-like repeats to the amino acid substitutions coincide with the EGF-like repeats known to have specific roles in *Notch* functions.

One potential cause disrupting the *Notch* activity in these *Notch* alleles is misfolding of Notch protein. It is known that misfolding of Notch leads to the depletion of Notch activity. Misfolding of Notch results in the abnormal intracellular distribution of Notch in epithelial cells. In wild-type epithelium, Notch localizes to the adherens

junctions (AJs). However, misfolding of Notch leads to its accumulation in the endoplasmic reticulum (ER) and absence from the AJs. In this study, subcellular distribution of Notch was examined in the epithelium of the embryonic hindgut in the *Notch* mutant alleles. Among 10 *Notch* mutant alleles that showed depletion of Notch signaling in lateral inhibition and inductive signaling, 6 alleles demonstrated the accumulation of Notch in the ER, which was coupled with the absence of Notch from the AJs. These results suggest that misfolding of Notch may account for the depletion of Notch activity in these 6 alleles. Moreover, I also found 3 *Notch* mutant alleles which showed normal subcellular localization of Notch, although *Notch* activity was abolished in them. Thus, I speculate that these mutations may disrupt some other functions of the EGF-like repeats essential for *Notch* activity, such as ligand binding and proteolytic cleavages of Notch.

Although the EGF-like repeats susceptible to induce misfolding of Notch upon the amino acid substitution were identified in this study, variety of amino acids substituted in each *Notch* mutant allele may affect the interpretation of the results. To exclude this possibility, I compared the results among 4 *Notch* mutant alleles that introduce an amino acid substitutions in the second cysteine to serine of the different EGF-like repeats. Such mutations are likely to reduce the stability of these EGF-like repeats by disrupting the

disulfide bridges. Profiles of all 4 alleles accord with the clusters of sensitive EGF-like repeats which were revealed here by the analyses including 19 alleles. Therefore, in despite of the limitation in the number of *Notch* alleles used in this study, the conclusions regarding the specificity of EGF-like repeats in the activity and folding of Notch were drawn with enough resolution.

In conclusion, this study provided evidences that the EGF-like repeats 8-10 and EGF-like repeat 25 may play crucial roles in the folding of whole Notch protein. This model should provide valuable insights into the future studies to understand the correlation between the structure and function of Notch.

Introduction

Cell signaling plays important roles in the regulation of various biological processes. In the last few decades, various cell signaling pathways were identified, and molecular mechanisms of these signal transductions were revealed. Among them, Notch signaling pathway has crucial roles in development and homeostasis across phylums (Artavanis-Tsakonas, et al., 1999, Gazave, et al., 2009). Through direct cell-cell interaction, Notch signaling regulates cell-fate specifications, cell physiology, apoptosis, and pattern formation (Bray, 2016). In addition, components of the Notch signaling

pathway are evolutionarily conserved (Artavanis-Tsakonas, et al., 1999, Gazave, et al., 2009). In accordance with the pivotal roles of Notch signaling in development and homeostasis in human, it is known that aberrant Notch signaling causes various diseases (Guruharsha, et al., 2012).

Major steps of Notch signaling cascade have been revealed (Bray, 2016). Notch receptor and its ligands, designated as DSL (Delta/Serrate/Lag-2) ligands, are single-pass transmembrane proteins (Baron, 2003). Upon the binding of DSL ligands to the extracellular domain of Notch, Notch undergoes two successive proteolytic cleavages by ADAM-family metalloproteases and γ-secretase (Bray, 2006). Consequently, Notch intracellular domain (NICD) is liberated from the plasma membrane and translocated into the nucleus where NICD forms a complex with CSL (CBF1/Suppresor of Hairless/Lag-1) transcription factors and promotes transcription from the target genes of Notch signaling (Figure 1) (Schweisguth, 2004, Bray, 2006, Hori, et al., 2013). However, in addition to these major steps in the activation of Notch signaling, there are complex regulatory processes lie behind this signaling cascade, which are also essential for Notch signaling transduction or involved in its finer tuning (Bray, 2016). For example, it has been shown that maturation of Notch involving folding and glycosylation in the endoplasmic reticulum (ER) and Golgi and endocytic trafficking of Notch are important

in the activation of Notch signaling (Yamamoto, et al, 2010, Rana, et al., 2011).

Notch has evolutionarily conserved domains, including Epidermal Growth Factor-like repeats (EGF-like repeats), NRR (negative regulatory region), Ankyrin-repeats, and PEST domain (Artavanis-Tsakonas, et al., 1999, Gazave, et al., 2009). In the extracellular domains of *Drosophila* Notch and mammalian Notch-1, there are 36 EGF-like repeats that serve as sites for *cis*- and *trans*-interactions with ligands (Figure 2) (Chillakuri, et al., 2012). The EGF-like repeats widely exist in the extracellular domains of various membrane proteins and play roles in extracellular events, such as cell adhesion, coagulation, and receptor-ligand interactions (Campbell & Bork, 1993, Downing, et al., 1996). They can be found in singular or in tandem units that are folded independently as individual folding modules (Wouters, et al, 2006). Additionally, the EGF-like repeats are also found in secretory factors, such as human epidermal growth factor receptor (EGFR) ligands family, including heparin-binding EGF-like growth factor (HBEGF), and human blood coagulation factors VII, IX, X, protein C, and thrombomoulin, in which the EGF-like repeats have adhesive functions (Figure 3, 4) (Wouters, et al., 2006, Tombling, et al., 2020).

A unit of EGF-like repeats generally consist of 30-40 amino acid residues that mostly form B-sheets structure including 6 conserved cysteines forming 3 disulfide bonds

in the following interactions: C1-C3, C2-C4, and C5-C6 (Figure 3,4,5,6) (Kelley, et al., 1987, Rand, et al., 1997, Wouters, et al, 2006, Haltom & Jafar Nejad, 2015, Tombling, et al., 2020, Mehboob & Lang, 2021). This disulfide bonds are found to give structural stability toward EGF-like repeats. Calcium ion (Ca^{2+}) binding also plays role in maintaining correct functions of Notch by stabilizing EGF-like repeats structure, and calcium binding EGF-like repeats are dispersed in 20 of 36 EGF-like repeats (Knott, et al., 1996, Feige, et al., 1998, Hambleton, et al., 2004). Such uneven distribution of the Ca^{2+}-binding EGF-like suggests some regional difference in the functions of Notch EGF-like repeats.

Protein glycosylation adds another layer of specificity to EGF-like repeats in Notch signaling because of specific glycan modifications present in various EGF-like repeats, including *O*-fucosylation, *O*-glucosylation, and *N*-glycosylation (Stanley & Okajima, 2010). These glycan modifications have unique and redundant roles in Notch signaling. For example, *O*-fucose glycan added to EGF-like repeats in the Notch ligand-binding site (EGF-like repeats 11–12) directly contributes to ligand–receptor interactions, as it lies within the binding pocket and modulates the specificity of the interaction between Notch and the two types of ligands, Delta and Serrate/Jagged (Luca, et al., 2015, Luca, et al.,2016). Although about two thirds of EGF-like repeats have some of these *O*-

fucose glycan modifications, the modifications are important only for specific EGF-like repeats, such as EGF-like 6, 8, 9, 12, and 36, in regulating Notch–ligand interactions (Kakuda & Haltiwanger, 2017, Pandey, et al., 2019). Thus, individual EGF-like repeats with *O*-fucose glycan modifications play specific roles. In addition, we previously reported that *O*-fucose and *O*-glucose glycans have redundant functions in folding Notch *in vivo* (Matsumoto, et al., 2016). In our previous study of *Drosophila* missense mutations in Notch EGF-like repeats, we revealed that Notch accumulates in the ER when *O*-fucose and *O*-glucose glycans are simultaneously removed, but not when either glycan alone is depleted (Matsumoto, et al., 2016). Since some of the EGF-like repeats lack the modification sites for these *O*-glycans, each EGF-like repeat likely differs in its response to the structural perturbation induced by depleting these glycans.

The uneven distributions of the EGF-like repeats with Ca^{2+}-binding and *O*-glycosylation sites in the tandem array of the 36 EGF-like repeats suggest that each EGF-like repeat and/or clusters of them may have specific functions in Notch signaling. Additionally, arrangement of the EGF-like repeats in *Drosophila* Notch and mammalian Notch-1 provided further evidence to support this idea. In the 36 EGF-like repeats of these two Notch proteins, an EGF-like repeat of any number from the N-terminal is most similar to the same number of the EGF-like repeats of another Notch paralog, compared with any

other EGF-like repeat in these two Notch proteins (Gazave, et al., 2009). This observation suggests that the alignment sequence of the EGF-like repeats is also important (Figure 3,6), suggesting that the EGF-like repeats have position-specific roles. However, specific roles of each EGF-like repeat and/or the clusters of them, for example in the proper folding and trafficking of Notch, remain unclear.

In previous studies, a collection of *Notch* mutants carrying amino acid substitution mutations were obtained by a genetic screen based on the bristle phenotypes of adult flies, which were observed in somatic clones generated by FLP-FRT system (Yamamoto et al., 2012). 18 *Notch* mutant alleles that have a single amino acid substitution in the different EGF-like repeats gave us an opportunity to study potential specificity of each EGF-like repeat in the activity, folding, and trafficking of Notch (Figure 7). Notch signaling is known to contribute to the three classes of signaling events: lateral inhibition, inductive signaling, and asymmetric cell division (Bray, 2016). The phenotypes of balding bristle, which were used to screen these *Notch* mutant alleles, are associated with the disruption of Notch signaling in asymmetric cell division and lateral inhibition of the peripheral nervous system (Figure 8) (Yamamoto, et al., 2012, Yamamoto et al., 2014, Haelterman et al., 2014). Thus, to reveal the distinct defects found in these *Notch* mutant alleles, analyses of the other classes of the Notch signaling events, such as

inductive signaling and lateral inhibition of central nervous system, may be informative. Neural hyperplasia of the embryonic central nervous system, designated as neurogenic phenotype, is a marker to evaluate the reduction of Notch signaling activity in lateral inhibition, because wild-type Notch signaling restricts the number of neuroblasts through lateral inhibition (Figure 9) (Sjopqvist & Andersson, 2017). In addition, Notch signaling also plays roles in inductive signaling, which can be analyzed by observing the boundary cells formed between the dorsal and ventral compartments of the hindgut epithelium in embryos (Figure 10) (Takashima, et al., 2002). Beside the advantage of the hindgut epithelium to analyze the inductive signaling, this tissue is also suitable for analyzing the intracellular localization of Notch (Takashima, et al, 2002). Wild-type Notch mostly localizes to the adherens junctions (AJs) in the epithelium, such as the epithelium of the embryonic hindgut (Sasaki, et al., 2007). It is known that defective folding of Notch results in the accumulation of Notch in the ER and the absence from the AJs (Okajima, et al., 2005). Furthermore, aberrant endocytosis of Notch can be revealed by the accumulation of Notch in endocytic compartments in epithelium (Okajima, et al., 2005, Yamamoto, et al., 2010, Hounjet & Vooij, 2021). Therefore, I presumed that the epithelium of embryonic hindgut is appropriate to study the defective folding and trafficking of Notch in the *Notch* mutant alleles.

Here, I systematically analyzed the collection of *Notch* mutant alleles to reveal their distinct defects of Notch signaling activity in lateral inhibition of the central nervous system and inductive signaling in the embryonic hindgut. Although these *Notch* mutant alleles were isolated based on the bristle phenotypes, which are associated with defective Notch signaling in asymmetric cell division, about half of them did not show the neurogenic phenotype and the failure in the induction of the boundary cells. These results suggested that these mutations of Notch affect Notch signaling in context-dependent manners, as reported in many Notch mutations in various contexts (Poellinger & Lendahl, 2008, Schwanbeck, et al., 2011). However, absent or normal activity of Notch signaling evaluated by these two phenotypes accorded with each other in all *Notch* mutant alleles examined. Upon amino acid substitution mutations, the EGF-like repeats that showed defects on folding and trafficking of Notch were found to form a cluster. Thus, these results suggest that each EGF-like repeat or clusters of them have specificity in their contributions to the folding and trafficking of Notch.

2. Materials and methods

2.1 *Drosophila* stocks and crosses

All experiments were performed at 25°C using a *Drosophila* standard culture

media. Canton-S was used as a wild-type control line. The collection of *Notch* mutants carrying missense mutations were provided by Dr. Shinya Yamamoto (Baylor College of Medicine, USA) (Yamamoto, et al., 2012, Haelterman, et al., 2014, Yamamoto, et al., 2014). The molecular lesions of these *Notch* mutants were revealed by previous genomic sequencing (Yamamoto, et al., 2012, Haelterman, et al., 2014, Yamamoto, et al., 2014). These *Notch* mutants were balanced with a balancer, *FM7c Kr>GFP* (Yamamoto, et al., 2012, Haelterman, et al., 2014, Yamamoto, et al., 2014).

The lines used for this experiment are N^{X} (DGRC 116669), $N^{Omicron}$ (DGRC 116715), N^{M} (DGRC 116748), N^{Jigsaw} (DGRC 116622), N^{Gamma} (DGRC 116750), N^{S} (DGRC 116605), N^{Iota} (DGRC 116608), N^{G} (DGRC 116671), $N^{Spl\text{-}1}$ (BDSC 182), N^{I} (DGRC 116689), N^{Zeta} (DGRC 116597), N^{H} (DGRC 116684), $N^{Ax\text{-}16}$ (BDSC 52014), N^{J} (DGRC 116700), N^{B} (DGRC 116625), N^{Q} (DGRC 116732), N^{Pi} (DGRC 116764), N^{Delta} (DGRC 116573), and N^{Lambda}, originally generated by Dr. Shinya Yamamoto. Each of these *Notch* mutants carries one amino acid substitution in the Notch protein (Yamamoto, et al., 2012, Haelterman, et al., 2014, Yamamoto, et al., 2014). N^{55e11} (BDSC 28813) was used as a null allele of *Notch*. *Pdi-GFP* (;;*Pdi-GFP*/*Pdi-GFP*) protein trap line was used to detect Protein disulfide isomerase, a typical marker of the ER (Roth & Pierce, 1987). To observe the Pdi-GFP in the epithelium of the embryonic hindgut, females

heterozygous for each *Notch* mutant (N^{mutant}/*FM7c Kr>GFP*) were crossed with males of *+/Y; ; Pdi-GFP/Pdi-GFP*. Male embryos hemizygous for each *Notch* mutant (N^{mutant}/Y) was selected based on their neurogenic phenotype and the absence of *FM7c Kr>GFP*.

2.2 Immunostaining

Embryos were observed by using antibody staining as previously described (Rhyu, et al., 1994). Confocal laser microscopy analysis was performed using LSM 700 (Zeiss) or LSM 810 (Zeiss) for obtaining high quality images, and the results were analyzed using LSM image browser and ImageJ software. Illustrative figures in this thesis were made using BioRender application. The following primary antibodies were used: rat anti-Elav (7E8A10, 1:500) (O'neill, et al., 1994), mouse anti-NICD (C17.9C6, 1:250) (Fehon, et al., 1990), mouse anti-Crumbs (Cq4, 1:250) (Tepass & Knust, 1993), rat anti-E-Cadherin (DCAD2 1:500) (Oda, et al., 1994), guinea pig anti-FL-Hrs (GP30, 1:1000) (Llyoid, et al., 2002), rabbit anti-Rab7 (1:5000) (Tanaka & Nakamura, 2008), rabbit anti-Rab11 (1:8000) (Tanaka & Nakamura, 2008), rabbit anti-GM130 (1:50, Abcam) (O'sullivan, et al., 2012), rabbit anti-GFP (1:250, 598 MBL) (Suzuki, et al., 2010), and rat anti-GFP (1:250, Nacalai Tesque)

The following secondary antibodies were used: Cy3-conjugated donkey anti-mouse (Jackson Immunoresearch), Cy5-conjugated anti-rabbit (Jackson

Immunoresearch), Cy-5 conjugated anti-rat (Jackson Immunoresearch), Cy5-conjugated anti-guinea pig (Jackson Immunoresearch), Alexa488-conjugated donkey anti-rat (Jackson Immunoresearch), and Alexa488-conjugated donkey anti-rabbit (Jackson Immunoresearch).

3. Results

3.1 Missense mutations introducing a single amino acid substitution in EGF-like repeats of Notch may be useful to understand the specificity of EGF-like repeats

Notch receptor is a type I single-pass transmembrane protein that consists of a large extracellular domain (about 200 kDa), a transmembrane domain, and an intracellular domain (about 100 kDa). The extracellular domain of *Drosophila* Notch consists of 36 EGF-like repeats and three lin-12/Notch repeats (LNR) (Bray, 2016). While, in the intracellular domain of *Drosophila* Notch, a RBPJ-associated module (RAM) domain, six Ankyrin repeats (ANK), a TAD/OPA domain, and a PEST domain reside (Figure 2) (Bray, 2016). These domains are conserved from *Drosophila* to human, and their specific functions were revealed in the regulations of *Notch* signaling (Bray, 2006).

Among these domains, the EGF-like repeats occupy the largest region in the Notch protein (Figure 2). Although these EGF-like repeats have a conserved structure

including 6 cysteines forming three definite disulfide bonds (Figure 3,4,5,6), previous studies suggested that each of EGF-like repeat and/or clusters of them may has functional specificities in the functions of *Notch*. However, such possibility has not been addressed by systematic approaches.

In order to examine the specific roles of each EGF-like repeat, I decided to utilize a collection of missense mutations of Notch that was established recently (Yamamoto, et al., 2012, Haelterman, et al., 2014, Yamamoto, et al., 2014). These *Notch* mutants carry a single missense mutation in the regions of genomic *Notch* locus corresponding to the EGF-like repeats and the transmembrane domain, which were previously confirmed by DNA sequencing (Yamamoto, et al., 2012, Haelterman, et al., 2014, Yamamoto, et al., 2014). Therefore, it becomes an advantage for me to reveal specific EGF-like repeats responsible for the phenotypes of these 19 *Notch* alleles (Yamamoto, et al., 2012). The numbers of EGF-like repeats and the amino acid substitution in each EGF-like repeat are summarized (Table 1, Figure 7). Furthermore, this collection includes 4 *Notch* mutants in which the second cysteine is replaced with serine in the different EGF-like repeats. Therefore, comparison of the phenotypes among these Notch mutations may allow us to detect some differences that imply functional specificities of these EGF-like repeats.

The missense mutations of Notch were isolated by genetic screen based on the

defects of bristles in somatic clone cells homozygous for each of *Notch* allele. *Notch* signaling controls the bristle formation at two major steps. First, the number of sensory organ precursors, each of which eventually form a single bristle, is restricted by Notch signaling through lateral inhibition. Second, cell-fates of cells constituting a bristle are determined by Notch signaling through the mechanisms of asymmetric cell division (Figure 8) (Schweisguth, 2015). Thus, this genetic screen covers Notch mutations that affect the lateral inhibition of the peripheral nervous system and asymmetric cell division. However, in addition to these functions, Notch signaling also plays crucial roles in lateral inhibition of the central nervous system and in inductive signaling in epithelial tissues (Bray, 2016). Thus, to reveal the distinct effects of these missense mutations of *Notch*, I thought that Notch signaling in these two processes should be analyzed in these *Notch* mutants. To analyze them in the collection of 19 missense mutants of *Notch*, the central nervous system and the hindgut of embryos were suitable (Cabrera, 1990 & Takashima, et al., 2002).

3.2 Only subset of the Notch missense mutations affects the development of embryonic nervous system

In *Drosophila* embryo, the central nervous system is formed from the neuroectoderm (Cau & Blader, 2009, Arefin, et al., 2019, Arefin, et al., 2020). In the

neuroectoderm, proneural clusters where all cells can differentiate into neuroblasts are formed. Once a cell chooses its cell-fate to become neuroblast, it starts to express high level of *Delta*, encoding a ligand for *Notch*, and activates Notch signaling in the neighboring cells, which leads to the suppression of their differentiation as neuroblasts. This process is referred to as lateral inhibition that restricts the number of neuroblasts as one third of cells in the neuroectoderm. The cells that fail to differentiate into neuroblasts in proneural clusters become epidermoblasts. Thus, in the absence of Notch signaling in the neuroectoderm, all cells in proneural clusters become neuroblasts at the expense of the epidermoblasts. This results in neural hyperplasia, designated as neurogenic phenotype (Figure 9).

In the embryonic central nervous system, depleted Notch signaling causes neural hyperplasia, designated as a neurogenic phenotype (Lehmann, et al., 1983). In this study, I observed neuronal cells by immunostaining with an antibody against the neuron-specific nuclear protein Elav (embryonic lethal abnormal vision) (Berger, et al., 2007). In wild-type embryos, anti-Elav stained the neuronal nuclei of the ladder-like nervous system (Figure 9); in contrast, the classic *Notch* amorphic (null) allele $Notch^{55e11}$ produced a severe neurogenic phenotype, with nearly the entire embryo stained by anti-Elav (Figure 9) (Lehmann, et al., 1983). Of the 19 *Notch* alleles tested, each carrying a different

missense mutation (Table 1), 10 had a neurogenic or brain deformation phenotype (Figure 9). Although the nature of brain deformation phenotype remained unclear, intensity of anti-Elav staining increased in these deformed brains, suggesting their neural hyperplasia that implies region-specific reduction of Notch signaling (Figure 9; Table 1). The remaining nine mutants exhibited a wild-type nervous system, even though the same alleles produced a Notch signaling-related phenotype in other contexts (Figure 9; Table 1) (Yamamoto, et al., 2012). Considering that the role of Notch signaling is context-dependent in various tissues and organs (Yamamoto, et al., 2012, Schweisguth, 2015), these missense mutations likely disrupt Notch signaling in a context-dependent manner.

3.3 Only the subset of missense mutations of Notch affects the formation of boundary cells in the hindgut

Next, I examined these *Notch* mutants for defects in boundary cells in the embryonic digestive system, since boundary cell formation is a typical example of inductive Notch signaling (Takashima, et al., 2002, Iwaki & Lengyel, 2002). The expression of the ligand Delta is limited to the ventral compartment of the hindgut because *engrailed*, which suppresses *Delta* expression, is expressed in the dorsal compartment (Takashima, et al., 2002). In the ventral cells where *Delta* is expressed, Notch signaling is suppressed in most cells by *cis*-inhibition of *Notch* via Delta

(Takashima, et al., 2002). However, since Delta presented from the ventral cells can signal Notch receptors expressed in the dorsal cells, where *cis*-inhibition does not take place, Notch signaling is activated in the single row of dorsal cells that subsequently differentiates into boundary cells (Takashima, et al., 2002).

Thus, I analyzed boundary cell formation to determine whether Notch signaling was disrupted in the *Notch* missense mutants during the development of the digestive system. The boundary cells highly express *crumbs*, which is required to establish apical-basal cell polarity and contributes to the organization of zonula adherens (Kumichel & Knust, 2014). When stained with an anti-Crumbs antibody, boundary cells were observed as two narrow bands, each composed of a single row of boundary cells (Figure 10) (Kumichel & Knust, 2014). I confirmed that *crumbs* expression is lost in embryos hemizygous for $Notch^{55e11}$ as previously described (Figure 10), demonstrating that my assay has sufficient sensitivity for my purposes (Takashima, et al., 2002). I assessed the presence or absence of boundary cells in embryos hemizygous for each *Notch* missense mutation and found that *crumbs* expression was depleted or showed abnormal gaps in 10 of the 19 *Notch* missense mutants (Figure 11; Table 1). However, the remaining nine missense mutations did not affect *crumbs* expression, indicating that inductive signaling was normal in this context (Figure 11; Table 1) (Yamamoto, et al., 2012). The 10 mutants

with defective inductive signaling were the same 10 mutants with neurogenic or brain deformation phenotype (Table 1). Therefore, I speculate that these 10 missense mutations are relatively severe loss-of-function alleles of *Notch*, whereas the other alleles are hypomorphic or context-dependent. I noticed that seven of these 10 mutations affect cysteine residues that form disulfide bonds and most of them are clustered in EGF-like repeats 8–10 (Table 1). Thus, Notch may be particularly sensitive to disruption of the basic structure of EGF-like repeats 8–10.

3.4 The EGF-like repeats of Notch have distinctive sensitivity to the structural perturbations induced by amino acid substitutions.

To compare the effect of these Notch mutations on inductive Notch signaling and lateral inhibition, I summarized the phenotypes of the boundary cells and central nervous system found in each Notch mutation (Table 1). I found that 10 out of 19 *Notch* alleles showed both the neurogenic or brain deformation phenotypes of the central nervous system and the depletion or abnormal gaps of *crumbs* expression in the embryonic hindgut. Thus, strikingly, defects on the lateral inhibition and inductive signaling coincided in all *Notch* alleles examined. Therefore, any of these *Notch* alleles did not show context-dependency in their phenotypes of the boundary cells and central nervous system in embryos. In contrast, although these *Notch* alleles were isolated based on bristle

phenotypes, which likely reflect abnormality of Notch signaling, 9 out of 19 *Notch* alleles did not show defects in the boundary cells or central nervous system in embryos. Since, Notch signaling is involved in the bristle formation through the control of asymmetric cell division, amino acid substitutions that occurred in these 9 *Notch* alleles may specifically affects the roles of *Notch* in asymmetric cell division, but not inductive signaling nor lateral inhibition.

My comparative analyses of phenotypes in the boundary cells and central nervous system in embryos also demonstrated a tendency that *Notch* mutant alleles introducing amino acid substitutions to the EGF-like repeats 8-10 and 25 showed loss-of-function phenotypes of *Notch* in the central nervous system and boundary cells in embryos. Thus, the EGF-like repeats 8-10 and 25 may be particularly sensitive to the perturbations introduced by these missense mutations.

3.5 *Notch* mutations carrying various amino acid substitutions in EGF-like repeats showed context dependent phenotypes

Notch mutations may disrupt Notch signaling by introducing defects in its folding or trafficking, which consequently results in the accumulation of Notch in the ER and/or endosomes (Okajima, et al., 2005). An accumulation of Notch in the ER can, in turn, lead to the loss of Notch from AJs in epithelial cells (Okajima, et al., 2005). This

loss is easily detected in the hindgut epithelium (Fuß & Hoch, 2002). Thus, I analyzed the subcellular localization of Notch in the hindgut epithelium of embryo hemizygous for each of the 19 *Notch* missense mutations, and found abnormal intracellular distribution of Notch in 8 of the 19 mutants (Figure 12 D–F,J–L,R,S; Table 2).

I compared signaling defects found in the central nervous system and boundary cells, assessed through *Notch* mutant phenotypes, with cellular defects related to Notch trafficking. I divided the *Notch* mutants accordingly into four classes based on the types of defects observed (Table 3), as follows: Class I comprised eight *Notch* mutants with normal Notch trafficking and normal *Notch* activity in the boundary cells and central nervous system. Class II comprised one *Notch* mutant that disrupted Notch trafficking but did not affect *Notch* activity in the boundary cells or nervous system. Class III comprised three *Notch* mutants that disrupted *Notch* activity in both the boundary cells and nervous system, but did not affect Notch trafficking. Class IV comprised seven *Notch* mutants that disrupted Notch trafficking and *Notch* activity in the boundary cells and nervous system. Based on these results, I conclude that a change in the amino acids in an EGF-like repeat can differ in its effect on Notch trafficking and activity, and that signaling defects and trafficking defects are not necessarily linked. Considering that amino acid substitutions in EGF-like repeats induced a range of defects in Notch trafficking and activities, the

specific amino acid sequences within certain EGF-like repeats are likely crucial for normal Notch activity and/or trafficking (Brennan, et al., 1997).

Typical examples of the defects in Notch trafficking found in Classes I to IV *Notch* mutant alleles are shown (Figure 13-16). Class I alleles include N^{Jigsaw} (EGF-8, V361M), N^{Pi} (EGF-9, D374G), N^{Alpha} (EGF-11, E452K), $N^{Spl\text{-}1}$ (EGF-14, I578T), N^{Lambda} (EGF-16, G668R), N^{I} (EGF-16, G671D), $N^{Ax\text{-}16}$ (EGF-29, G1174A), and N^{J} (EGF-34, C1567S) (Figure 13). In these parentheses, the left shows the numbers of the EGF-like repeats from the N-terminus (EGF-number), and the right shows the substituted amino acid at the position shown in number from the N-terminus. Class I alleles were isolated based on their balding or reduced bristle phenotype, suggesting the disruption of Notch signaling in asymmetric cell division. Nevertheless, class I alleles did not show defects in the embryonic neurogenesis or boundary cell formation. These results suggest that amino acid substitutions found in class I mutants affect asymmetric cell division but not lateral inhibition nor inductive Notch signaling. Previous studies may explain this observation. For example, it was previously shown that N^{jigsaw} mutant affects preferences of binding between Notch and either one of two ligands (Yamamoto, et al., 2012). In this mutation, Notch preferentially binds to Delta rather than Serrate, leading to the defect of inductive Notch signaling in the wing imaginal disc (Yamamoto, et al., 2012). Thus, it is

speculated that the EGF-like repeat 8 may function to facilitate the binding to Serrate (Yamamoto, et al., 2012). However, in the embryonic nervous system and the boundary cells, it is known that Serrate ligand is dispensable, and Delta acts as primary ligand to activate *Notch* (Takashima, et al, 2002, Moore & Alexandre, 2020). This may explain that N^{jigsaw} mutant did not show phenotypes in the embryonic nervous system and the boundary cells. Furthermore, $N^{Spl\text{-}1}$ mutant that has an amino acid substitution in the EGF-14 was known to have a rough eye phenotype and abnormal bristle formation (Brennan, et al., 1997). It was previously suggested that the rough eye phenotype is caused by an impaired cell-adhesion mediated by *Notch*. Therefore, $N^{Spl\text{-}1}$ mutant may affect a different aspect of *Notch* function from its roles in lateral inhibition and inductive signaling. In addition, $N^{Spl\text{-}1}$ mutant showed increased *Notch* activity in some tissues, although in the eye and bristle it is thought to be a loss-of-function mutation (Lieber, et al., 1992, Brennan, et al., 1997, Nagel & Preiss, 1999). Thus, behavior of $N^{Spl\text{-}1}$ shows complex context-dependencies, which is also found in my study.

3.6 A trafficking defect of Notch was not always coupled with a loss of *Notch* activity

The only Class II mutant in this study, N^{H}, carries an amino acid substitution in the 29th EGF-like repeat with a cysteine (C) to serine (S) amino acid substitution at the 1155th amino acid residue (EGF-29, C1155S); this mutation affected the intracellular

trafficking of Notch but not *Notch* function in lateral inhibition or inductive signaling in embryogenesis (Figures 14). Notch was not detected in AJs in the hindgut of N^H hemizygote embryos, where Notch is highly enriched in wild-type flies, but was instead found in punctate structures in the cytoplasm. To reveal the nature of such punctae, I analyzed the potential colocalization of Notch with markers of various intracellular compartments. I found that Notch colocalized with the early endosome marker Hrs (Hepatocyte growth factor regulated tyrosine kinase substrate) in the hindgut epithelium of N^H hemizygote embryos (Figure 18) but not wild-type embryos (Figure 18; Table 2). On the other hand, Notch did not colocalize with markers for the ER (PDI-GFP) (Figure 18), *cis*-Golgi, recycling endosomes, or late endosomes under the same conditions (Figure 22-26). Therefore, in N^H hemizygotes, Notch is absent from AJs and accumulates in early endosomes in the hindgut epithelium, although such mislocalization of Notch does not appear to affect Notch signaling activity in this context. Under this condition, Notch presented at the plasma membrane appeared to be severely reduced, whereas the activity of Notch signaling was maintained normally. I speculated that this phenomenon can be explained by the nature of the N^H mutation, which introduces an amino acid substitution in EGF-like repeat 29, included in the Abruptex domain (Yamamoto, 2020). Since mutations in the Abruptex domain often result in gain-of-function *Notch* alleles

(Yamamoto, 2020), it is possible that N^{H} encodes a gain-of-function *Notch* while simultaneously reducing Notch presentation at the plasma membrane, which should reduce Notch signaling activity. Therefore, I speculate that a balance of these opposing effects on *Notch* activity belonging to the N^{H} mutation may account for my observation that Notch signaling activity was normal in this mutant.

3.7 Some amino acid substitutions disrupt Notch signaling without affecting the trafficking of Notch

Conversely, my analyses revealed that the Class III alleles N^{Delta} (EGF-9, D389N), N^{G} (EGF-13, C535S), and N^{B} (TMD, I1751K) showed attenuation in *Notch* activity in lateral inhibition, as predicted from brain deformation phenotype, and in inductive signaling (Figure 15) during embryogenesis, whereas Notch trafficking was normal in the hindgut epithelium (Figure 15). These results suggest that the disruption of *Notch* activity is not always coupled with Notch trafficking defects. Considering the many factors that regulate Notch signaling at various layers within a cell, I speculate that these *Notch* missense mutations might disrupt some processes other than normal Notch trafficking. For example, N^{Delta} and N^{G} might disrupt ligand-receptor binding, since these mutations introduce amino acid substitutions into EGF-like repeats 9 and 13, respectively.

Meanwhile, N^{B} allele carries a mutation introducing an amino acid substitution

into the transmembrane domain (TMD) in Notch. I speculated that the mutation may affect the S3 cleavage, which occurs at the proximal of TMD and is essential for the activation of *Notch*.

3.8 In various *Notch* missense mutations, trafficking defects of Notch couple with loss of *Notch* activity

In total, 7 of the 19 *Notch* mutant alleles tested were Class IV, which exhibit trafficking defects and loss of *Notch* activity in both neural development and the formation of hindgut border cells (Figure 16; Table 3). The Class IV mutants include N^{X} (EGF-8, C343S), $N^{Omicron}$ (EGF-8, C343Y), N^{Q} (EGF-8, D331N), N^{Gamma} (EGF-9, C398Y), N^{S} (EGF-9, C407S), N^{Iota} (EGF-10, C413S), and N^{Zeta} (EGF-25, C993S). Notch was absent from AJs in all Class IV alleles (Figure 17). Six of the seven Class IV mutants produced Notch proteins that accumulated in the ER, as shown by colocalization studies with Pdi-GFP (Figure 17), whereas hardly any Notch was detected in this organella in wild-type embryos (Figure 17). On the other hand, Notch proteins derived from these six mutants did not colocalize with markers of other intracellular compartments, such as *cis*-Golgi, early endosomes, recycling endosomes, late endosomes, or AJs (Figure 22-26). Previous studies show that misfolded Notch protein was not transported to AJs because it was trapped in the ER (Matsumoto, et al., 2016, Okajima, et al., 2005). These six mutants

may also produce misfolded Notch that is not exported from the ER.

Importantly, I found that six of the seven Class IV mutants have amino acid substitutions in EGF-like repeats 8–10. Thus, the EGF-like repeats in this region may be especially sensitive to structural perturbations (Figure 19). I speculate that these three EGF-like repeats may be particularly important in folding the whole extracellular domain of Notch.

The Class IV mutant N^{Zeta}, which has an amino acid substitution in EGF-like repeat 25, accumulates Notch in the ER, suggesting that the mutation induces a severely misfolded product. EGF-like repeat 25 is a part of the Abruptex domain (EGF-like repeats 24–29) (De Celis & Bray, 2000). Amino acid substitutions within the Abruptex domain are known to induce gain-of-function mutations of *Notch*, suggesting that the Abruptex domain is involved in suppressing *Notch* activation (De Celis & Bray, 2000). It has also been suggested that the Abruptex domain contributes to forming Notch dimer proteins (Pei & Baker, 2008). Given the apparent sensitivity of EGF-like repeat 25 to structural perturbation (Figure 19), the Abruptex domain may also be involved in the high-order organization of EGF-like repeats.

3.9 Disruptions of conserved disulfide bonds in different EGF-like repeats induce distinctive defects in *Notch* activity and trafficking

Although I observed different phenotypes associated with amino acid substitutions in individual EGF-like repeats, some differences may depend on the specific amino acids that replace the original residue rather than the position of the repeat. Four of the *Notch* missense mutants tested here, N^{X} (EGF-8, C343S), N^{G} (EGF-13, C535S), N^{Zeta} (EGF-25, C993S), and N^{H} (EGF-29, C1155S), have the same amino acid substitution at the conserved second cysteine though occurring in different EGF-like repeats, and these cysteines were replaced with serine residues. Considering the differences in the behavior of these variants in my assay system, my data argue that, at least among the mutants I tested, the matter of which EGF-like repeat contains the mutation has important biological consequences (Figure 20). These results also suggest that my analysis of the defects induced in the various mutants also indicate, at least to some degree, a specific function of the EGF-like repeats containing the amino acid substitutions. On the other hand, my analyses also revealed that the N^{G} (EGF-13, C535S) and N^{J} (EGF-34, C1341Y) mutants, which have amino acid substitutions at conserved cysteines, did not accumulate Notch in the ER (Figure 12). This observation suggests that these EGF-like repeats are tolerant to

structural perturbation with consequent misfolding. This also supports my idea that each EGF-like repeat plays specific roles in Notch folding.

Discussion

Notch has 36 EGF-like repeats in its extracellular domain (Artavanis-Tsakonas, et al., 1999). Although these EGF-like repeats share a conserved structure, they play diverse roles as individual repeats and as clusters (Bray, 2016). For example, EGF-like repeats 11–12 form the core ligand-binding site (Rebay, et al., 1991). EGF-like repeats 10–12, 11–12, and 8 specifically contribute to *cis*-inhibition (Becam, et al., 210), *trans*-activation (Chillakuri, et al., 2012), and ligand selection (Yamamoto, et al., 2012), respectively. Genetic evidence suggests that EGF-like repeats 24–29, designated as the Abruptex domain, negatively regulate the Notch receptor (De Celis & Bray, 2000, Baron, 2017, Yamamoto, 2020). However, relatively little is known about the specific roles of individual EGF-like repeats, and a complete high-order structure of Notch and its 36 EGF-like repeats in action has not been solved through structural analysis. In this study, I attempted to reveal the specific contributions of each EGF-like repeat to the activity, folding, and intracellular trafficking of Notch by studying the effect of missense mutations.

I analyzed 19 *Notch* mutants carrying missense mutations that were identified through a recent forward genetic screen (Yamamoto, et al., 2012) or as classic alleles. These mutations introduce unique amino acid substitutions into EGF-like repeats in 18 cases, and into the transmembrane domain in one case (Yamamoto, et al., 2012). The mutants collected through genetic screening were isolated by clinical observation of *Notch*-related phenotypes in the bristles (Yamamoto, et al., 2012). To further characterize these mutants, I examined two other well-studied Notch-related phenotypes in embryonic tissues: lateral inhibition during central nervous system development and inductive signaling during boundary cell formation in the hindgut (Table 1). My comparative analyses revealed that 10 out of 19 alleles exhibited either a neurogenic or brain deformation phenotype and boundary cells abnormalities (Table 1). In all cases, these two defects were observed coincidently. Therefore, the behavior of each of these 10 missense mutations was the same for lateral inhibition and for inductive signaling during embryogenesis. Although context dependency in Notch signaling has been studied extensively, it is still difficult to explain how it operates differently in various tissues (Siebel & Lendahl, 2017). Clear differences and similarities in the behaviors of the *Notch* missense mutants observed in this study provide an excellent opportunity to understand the molecular mechanisms of context-dependent *Notch* signaling.

As summarized in Figure 19, my analysis revealed that the EGF-like repeats sensitive to the amino acid substitutions with respect to the depletion of *Notch* activity are found in two regions within the 36 EGF-like repeats. One of these regions is EGF-like repeats 8–10, as revealed in the *Notch* missense mutants N^{X}, $N^{Omicron}$, N^{Q}, N^{Gamma}, N^{S}, and N^{Iota}. Intriguingly, the importance of EGF-like repeats 8-10 agrees with previous findings. For example, *O*-fucose modifications on EGF-like repeats 8 and 12 in Notch1 engage the EGF-like repeat 3 and the C2 domain, respectively, of the Jagged1 ligand (Luca, et al., 2017). Moreover, EGF-like repeat 8 modulates ligand binding selectivity in *Drosophila* (Yamamoto, et al., 2012). EGF-like repeats 8-10 of Notch1 are required for DLL1- and DLL4-induced Notch signaling (Andrawes, et al., 2013). The importance of EGF-like repeats 8-10 has also been shown by analyzing *O*-fucose glycan modifications. *O*-fucose glycan modifications in EGF-like repeats 8, 9, and 12 of *Drosophila* Notch and in EGF-like repeats 8 and 12 of Notch1 specifically play important roles in modulating Notch-ligand binding (Pandey, et al., 2019, Kakuda & Haltiwanger, 2017). Collectively, these results highlight the importance of EGF-like repeats 8-10 in Notch functions.

Another sensitive region was found in the EGF-like repeat 25, although this region was identified based on only one *Notch* mutant, N^{zeta}. This region overlaps with the Abruptex domain (EGF-like repeats 24-29), which is known to negatively regulate

Notch activity (De Celis & Bray, 2000). Genetic interaction analysis suggests that the Abruptex domain can be divided into two different clusters, EGF-like repeats 24-25, known as "suppressor of *Notch*", and EGF-like repeats 27-29, known as "enhancer of *Notch*" (Yamamoto, 2020). The precise molecular function of Abruptex domain is unknown, and it is not clear why the N^{zeta} mutation found in this region leads to a loss-of-function rather than a gain-of-function *Notch* phenotype. A more detailed study of this mutation along with other *Abruptex* alleles of *Notch* will likely provide insights into this mysterious domain. In summary, these two missense-sensitive clusters of EGF-like repeats correspond well to the EGF-like repeats that have been shown to play specific roles in *Notch* functions.

My results also revealed that of seven *Notch* mutants with an amino acid substitution in one of the sensitive clusters, six accumulated Notch abnormally in the ER of the hindgut epithelium. I found seven Class IV Notch mutations in this study— N^{X}, $N^{Omicron}$, N^{Q}, N^{Gamma}, N^{S}, N^{Iota}, and N^{Zeta}, which disrupted Notch trafficking and *Notch* activity (Table 3). Notch misfolding is known to cause Notch to accumulate in the ER (Okajima, et al, 2005). Therefore, I speculated that amino acid substitutions in the EGF-like repeats of the sensitive clusters may induce global misfolding of Notch, which prevents the export of Notch from the ER by quality control mechanisms (Matsumoto, et

al., 2016, Okajima, et al., 2005). On the other hand, in Class III mutants, including N^{Delta}, N^{G}, and N^{B}, Notch trafficking was normal, although *Notch* activity was reduced. However, in Class III mutants, defects in neural development were observed only in the brain, but not in the other part of the central nervous system. Considering that all Class IV mutants showed neurogenic phenotype in the entire central nervous system, underlying defects in Notch signaling may be different between Class III and Class IV, although all of them showed defects in inductive Notch signaling, as judged by the disruption of boundary cell formation. It is known that the activation of Notch signaling requires several steps in addition to proper Notch folding, such as ligand binding and Notch processing. Therefore, I speculate that some of these other steps might be disrupted in the Class III mutants, which may also explain the difference of neuronal phenotypes between Class III and Class IV.

As a potential limitation of this study, one could argue that the type of amino acid substitution found in the *Notch* mutants might be more important than which EGF-like repeat is affected. However, my analysis of the missense mutations in the *Notch* mutants N^{X}, N^{G}, N^{Zeta}, and N^{H}, which introduce the same amino acid substitution in the conserved second cysteine to serine, but in different EGF-like repeats, argues that identical amino acid changes introduced into different EGF-like repeats can differ in

effect. Therefore, despite the limitation in the number of *Notch* alleles used here, my analyses successfully demonstrate, at least to some extent, the specificity of individual EGF-like repeats in Notch folding and activity.

Based on the results of my study, I propose that the EGF-like repeats 8-10 and 25 are particularly susceptible to structural perturbation with consequent misfolding and inactivation of Notch. I speculate that the ER may monitor the folding of these particular EGF-like repeats more strictly than other repeats because of their critical roles in Notch receptor functions. This idea should provide insights for further studies of correlations between Notch structure and function, and may provide molecular handles to assist in the functional interpretation of the missense variants that are found in human Notch receptors and are linked to diverse genetic disorders or cancers.

Figures and tables

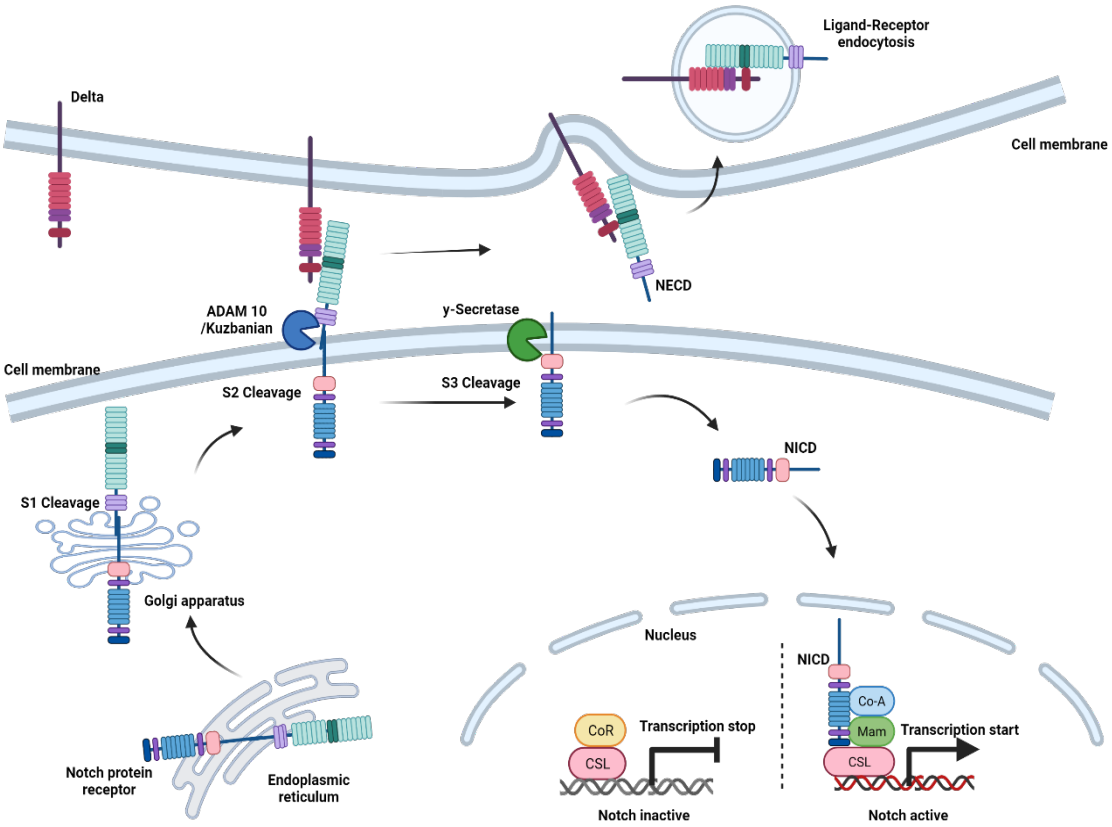

Figure 1. Notch signaling pathway.

Notch is a type 1 transmembrane receptor and needs to bind to the ligand (Delta or Serrate) to initiate the activation of the Notch signaling pathway. Major steps of the Notch pathway have been understood. Starting from Notch synthesized in the ER, it is cleaved at the S1 site (S1 cleavage) in the Golgi. Upon binding to the ligand, Notch undergoes two subsequent cleavages (S2 and S3 cleavages), leading to the release of Notch intracellular domain (NICD) from the plasma membrane. Consequently, NICD is translocated into the nucleus where it initiates transcription of Notch signaling target genes.

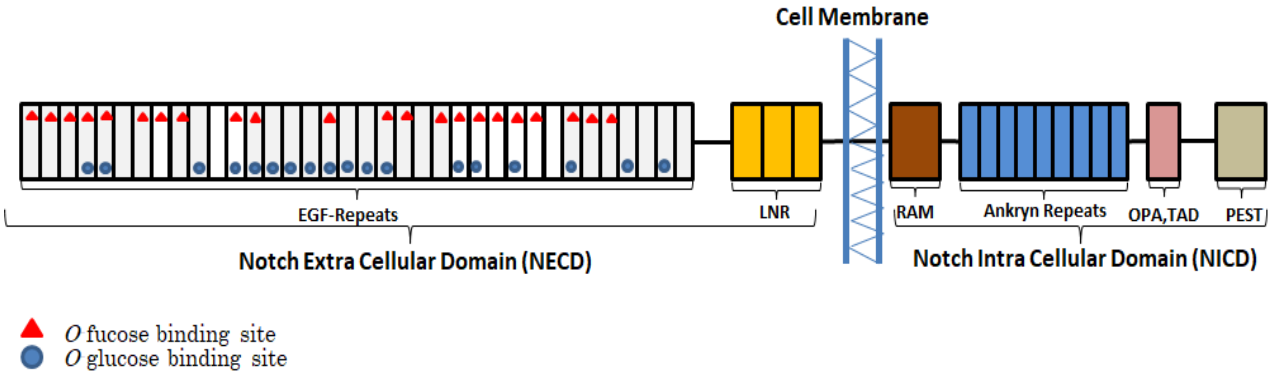

Figure 2. The Notch receptor

Notch consists of a large extracellular domain (about 200 kDa), a transmembrane domain, and an intracellular domain (about 100 kDa). In the extracellular domain of *Drosophila* Notch, 36 EGF-like repeats and three lin-12/Notch repeats (LNR) are present. In the intracellular domain, a RBPJ-associated module (RAM) domain, six Ankyrin repeats (ANK), a TAD/OPA domain, and a PEST domain resides. Subset of these EGF-like repeats has consensus sequences of *O*-fucosylation (red triangle) and/or *O*-glucosylation (blue circle), and about one third of the EGF-like repeats do not have these *O*-glycan modifications.

Figure 3. Amino acid sequence homology found in various EGF-like repeats

Sequence alignment of various EGF-like repeats. 6 conserved cysteines (C1-C6) in each EGF-like repeat are indicated by black boxes. Amino acid sequences of *Drosophila* Notch EGF-1 (the first EGF-like repeat from the N-terminal), Human Notch1 EGF-1, Human Thrombomodulin EGF-1, Human Coagulation Factor 9 EGF-1, and *Xenopus* Notch homolog, Xotch1 EGF-1 are shown.

Rao, et al., 1996

X-ray structure from Human coagulation factor IX EGF-1 (a.a. 92-130)

Figure 4. Structure of Human coagulation factor IX EGF-1

X-ray structure of Human coagulation factor IX EGF-like repeat 1 (the first EGF-like repeat from the N-terminal). It has 6 conserved cysteines as mentioned in Figure 3. The tertiary structure of this EGF-like repeat is conserved in other EGF-like repeats, in which two stranded B-sheet structure known as major (N-terminal) and minor (C-terminal) is observed (Wouters, e al., 2005)

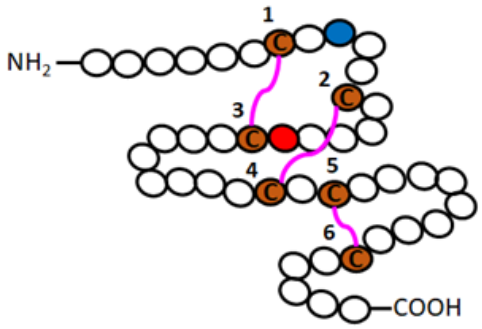

Illustration drawing of a typical EGF-like repeat in *Drosophila* Notch

EGF 11
(a.a. 449-486)

EGF 12
(a.a. 488-524)

EGF 13
(a.a. 526-562)

Suckling, et al., 2020

X-ray structure of the EGF-like repeats 11-13 from *Drosophila* Notch

Figure 5. Structure of *Drosophila* Notch EGF-repeats in the ligand-binding region

Upper:

An EGF-like repeat consists of 30-40 amino acids including 6 cysteines (indicated by C in brown circles) that form three definite disulfide bonds that define its three-dimensional structure. Red circle is the site for *O*-fucosylation with the consensus sequence (C2-*X*-*X*-*X*-*X*-(S/T)-C3), and blue circle is the site for *O*-glucosylation with the consensus sequence (C1-*X*-*S*-*X*-(P/A)-C2).

Below:

X-ray structure of the EGF-like repeats 11-13 from *Drosophila* Notch encompassing the EGF-like repeats 11 (a.a. 449-486), 12 (a.a. 488-524), and 13 (a.a. 526-562). These regions cover the ligand binding site in EGF 11 and 12, which are important for binding between Notch and ligands. EGF-like repeats share a common tertiary structure as two stranded B-sheets. This structure appears in each of EGF-like repeat.

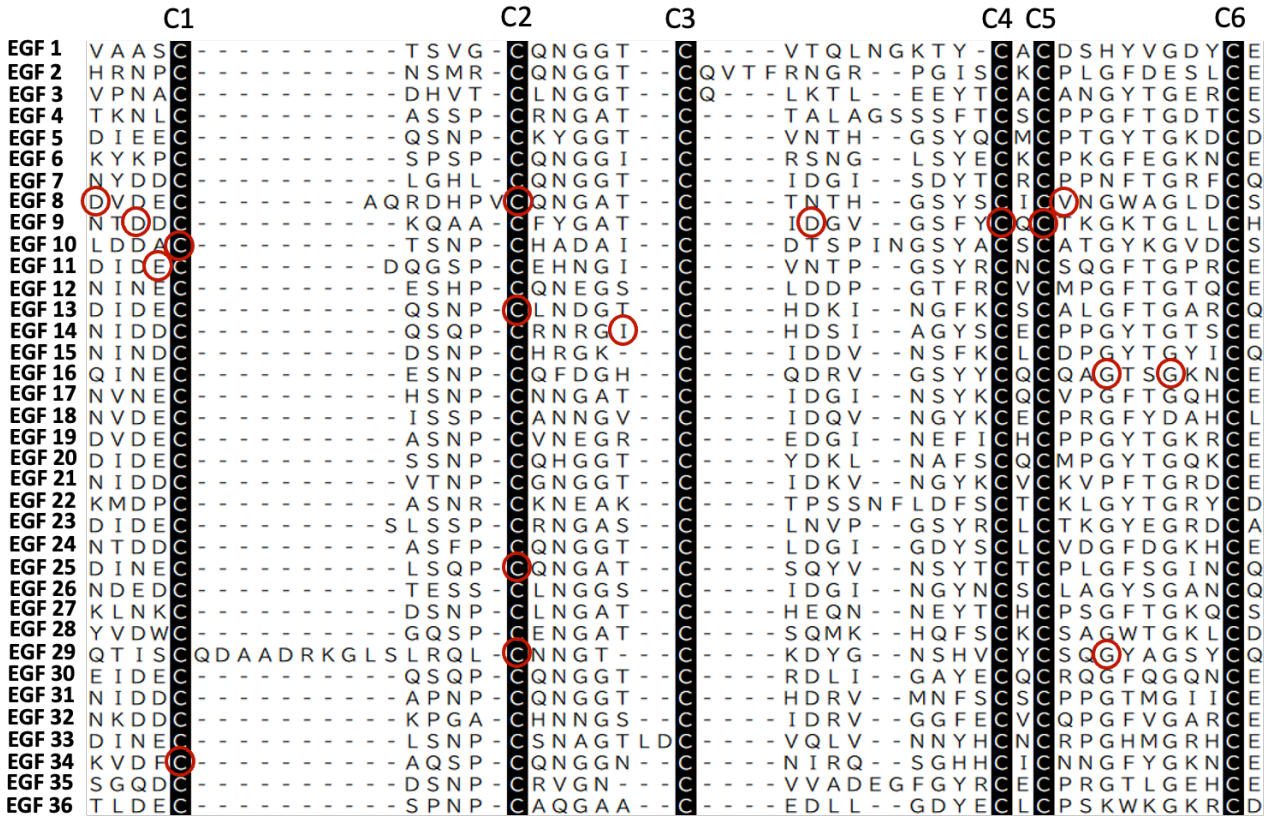

Figure 6. Amino acid sequence of *Drosophila* Notch EGF-like repeats

Amino acid alignment of sequences from *Drosophila* Notch EGF-like repeats 1-36 (Kelley, et al., 1987, Adams, et al., 2000). The 6 conserved cysteines in each of the EGF-

like repeat are shown as C in black boxes. Red circles show the positions of amino acids changed in the *Notch* mutant alelles

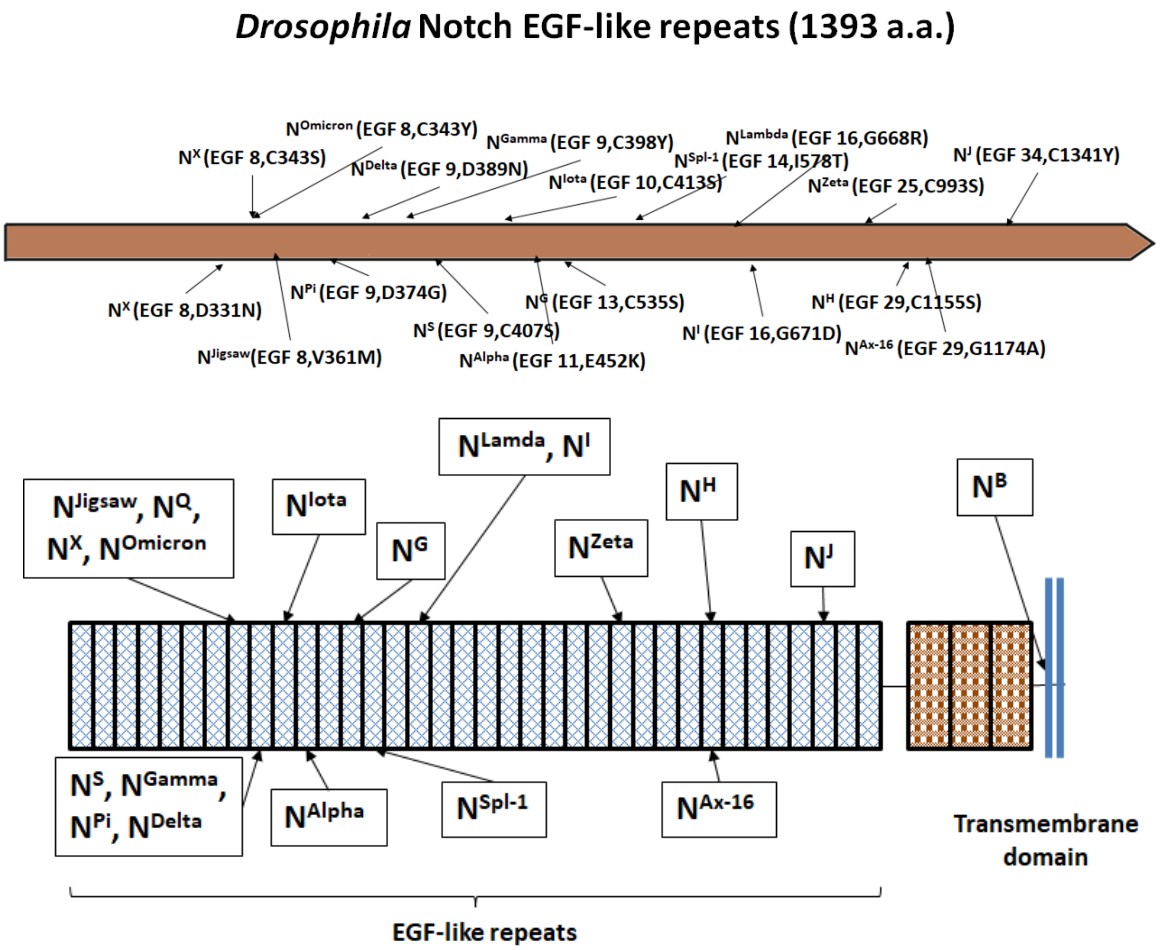

Figure 7. Position of the EGF-like repeats with amino acid substitutions in *Notch* mutant alleles analyzed in this study

Position of the EGF-like repeats with a missense mutation in 18 *Notch* mutants are shown. N^{B} has a missence mutation in the sequence corresponding to the transmembrane domain (Yamamoto, et al., 2012). In parentheses, the positions of the EGF repeats are showed in left, and amino acid numbers and substituted amino acids are showed in right)

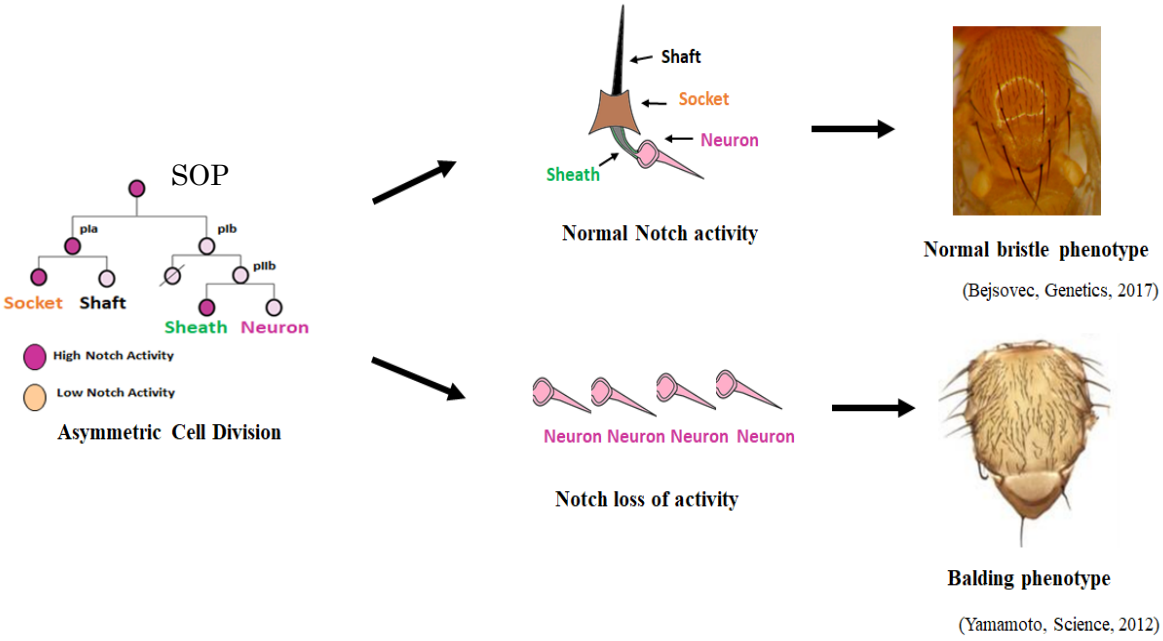

Figure 8. Bristle formation and asymmetric cell division in *Drosophila*

Notch signaling controls the bristle formation at two major steps. First, the number of sensory organ precursors (SOP), which eventually forms a single bristle, is restricted by Notch signaling through lateral inhibition. Second, the cell-fates of cells constituting a bristle are determined by Notch signaling through the mechanisms of asymmetric cell division (Schweisguth, 2015). A sensory organ precursor will differentiate into four different cells, a shaft, socket, sheath, and neuron, which depends on the activity level of Notch during asymmetric cell division. However, in loss-of-function mutations of *Notch*, a sensory organ precursor produced in four neurons, which results in loss of the bristle, called balding phenotype.

No	Name	EGF-like Repeat	Mutation Position	*Notch* Activity		
				Bristle Formation	Lateral Inhibition	Inductive Signaling
1	N^{X}	EGF 8	C343S (C_2S)	Absent	Neurogenic	Depletion
2	$N^{Omicron}$	EGF 8	C343Y (C_2Y)	Absent	Neurogenic	Depletion
3	N^{Q}	EGF 8	D331N	Absent	Neurogenic	Depletion
4	N^{Jigsaw}	EGF 8	V361M	Normal	Normal	Normal
5	N^{Pi}	EGF 9	D374G	Absent	Normal	Normal
6	N^{Delta}	EGF 9	D389N	Absent	Brain deformation	Depletion
7	N^{Gamma}	EGF 9	C398Y (C_5Y)	Absent	Neurogenic	Depletion
8	N^{S}	EGF 9	C407S (C_6S)	Absent	Neurogenic	Depletion
9	N^{Iota}	EGF 10	C413S (C_1S)	Absent	Neurogenic	Depletion
10	N^{Alpha}	EGF 11	E452K	Absent	Normal	Normal
11	N^{G}	EGF 13	C535S (C_2S)	Absent	Brain deformation	Depletion
12	N^{Spl-1}	EGF 14	I578T	Reduced	Normal	Normal
13	N^{Lambda}	EGF 16	G668R	Absent	Normal	Normal
14	N^{I}	EGF 16	G671D	Absent	Normal	Normal
15	N^{Zeta}	EGF 25	C993S (C_2S)	Absent	Neurogenic	Depletion
16	N^{H}	EGF 29	C1155S (C_2S)	Absent	Normal	Normal
17	N^{Ax-16}	EGF 29	G1174A	Reduced	Normal	Normal
18	N^{J}	EGF 34	C1341Y(C_1Y)	Absent	Normal	Normal
19	N^{B}	TMD	I1751K	Normal	Brain deformation	Abnormal Gaps

Table 1. List of *Notch* mutant alleles examined in this study

19 *Notch* mutant alleles examined in this study are listed. All mutants carry single missense mutations that introduce amino acid substitutions in the EGF-like repeats (1-18) or the transmembrane domain (19) are listed in the column of "Name" (Yamamoto, et al., 2012). The positions of EGF-like repeats with amino acid substitutions are shown as the

numbers of the EGF-like repeats from the N-terminal in the column of “EGF-like repeat”. The nature of amino acid substitutions is shown in the column of “Mutation Position”. Notch activity analyzed based on “Bristle Formation”, “Lateral inhibition”, and “Inductive Signaling” are shown. “Absent” indicates the missing of bristles. “Reduced” indicates the reduced number of bristles. “Neurogenic” indicates the neural hyperplasia in the embryonic nervous system. “Brain deformation” indicates abnormal brain development. “Depletion” indicates the missing of the boundary cells in the embryonic hindgut. “Abnormal gaps” indicates the partial missing of the boundary cells in the embryonic hindgut

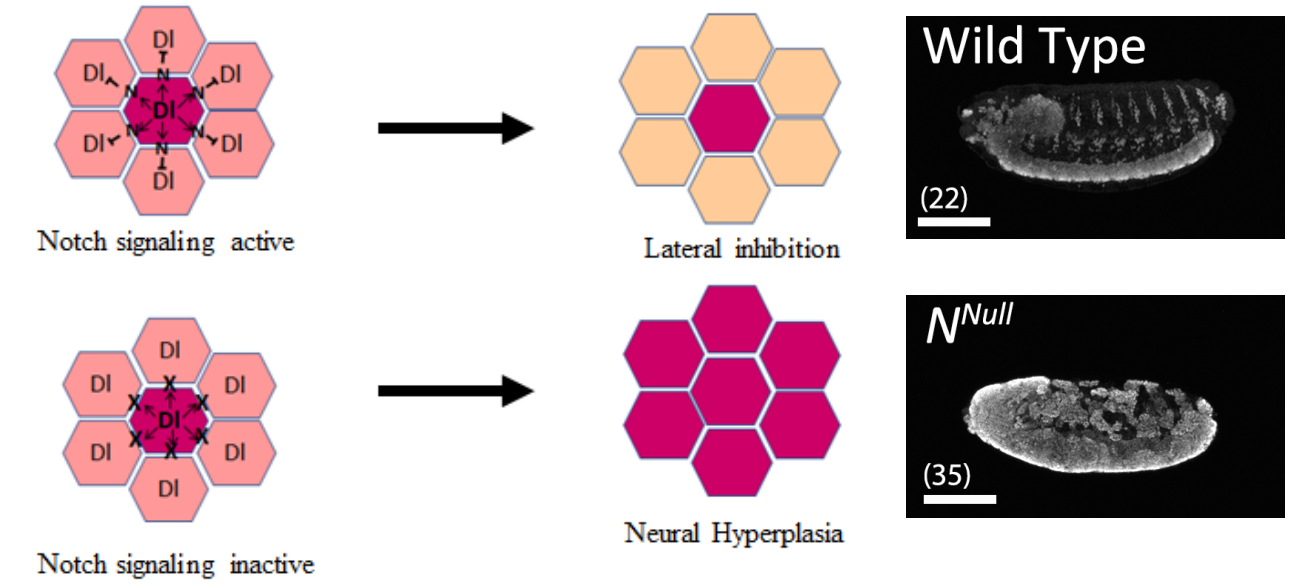
Dl
N
Notch signaling active
Lateral inhibition
Wild Type
(22)
X
Notch signaling inactive
Neural Hyperplasia
N^Null
(35)

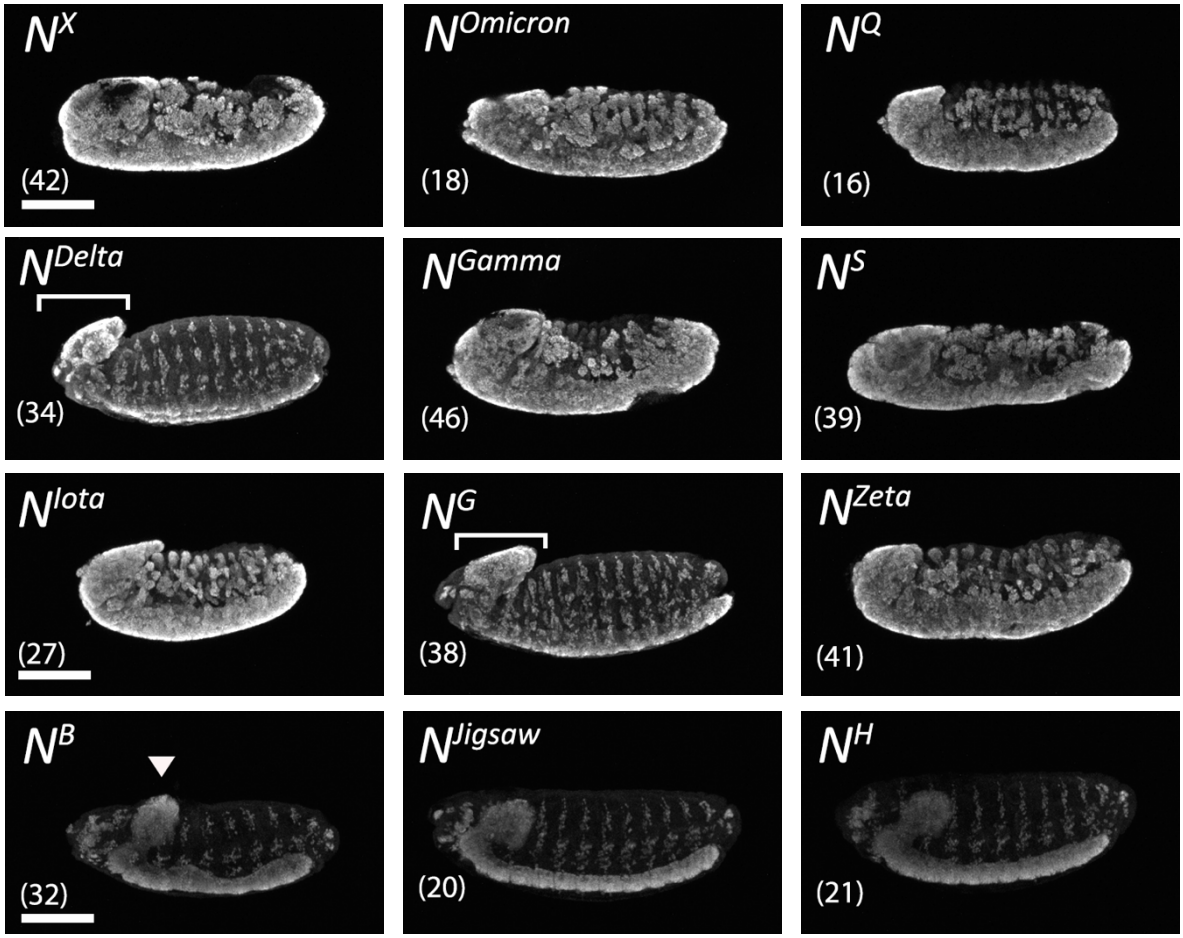
N^X
(42)
N^Omicron
(18)
N^Q
(16)
N^Delta
(34)
N^Gamma
(46)
N^S
(39)
N^Iota
(27)
N^G
(38)
N^Zeta
(41)
N^B
(32)
N^Jigsaw
(20)
N^H
(21)

Scale: 100 μm

Figure 9. 10 out of 19 *Notch* mutant alleles showed neurogenic phenotype that indicates the failure in lateral inhibition

Top:

Drosophila central nervous system is formed from the neuroectoderm in which proneural clusters are formed. All cells in a proneural cluster are capable of differentiating into neuroblasts. However, once a cell chooses its cell-fate to neuroblast (magenta), it starts to express high level of *Delta*, encoding a ligand for *Notch*, and activates Notch signaling in the neighboring cells, leading to the suppression of their differentiation as neuroblasts (cream color). However, in the absence of Notch signaling, all cells in proneural clusters become neuroblasts, which results in neural hyperplasia, designated as neurogenic phenotype.

Bottom:

To observe the nervous system, embryos were stained with an anti-Elav antibody (white). The names of *Notch* mutant alleles are shown in the upper left. numbers shows the numbers of embryos analyzed. N^{X}, $N^{omicron}$, N^{Q}, N^{Gamma}, N^{S}, N^{Iota}, and N^{zeta} showed neurogenic phenotype. N^{Delta}, N^{G} and N^{B} showed brain deformation (shown with white white brackets). 10 out of 19 mutants showed either neurogenic or brain deformation phenotype, while the rest of them have wild-type nerve system (as examples in N^{Jigsaw} and

N^H mutants).

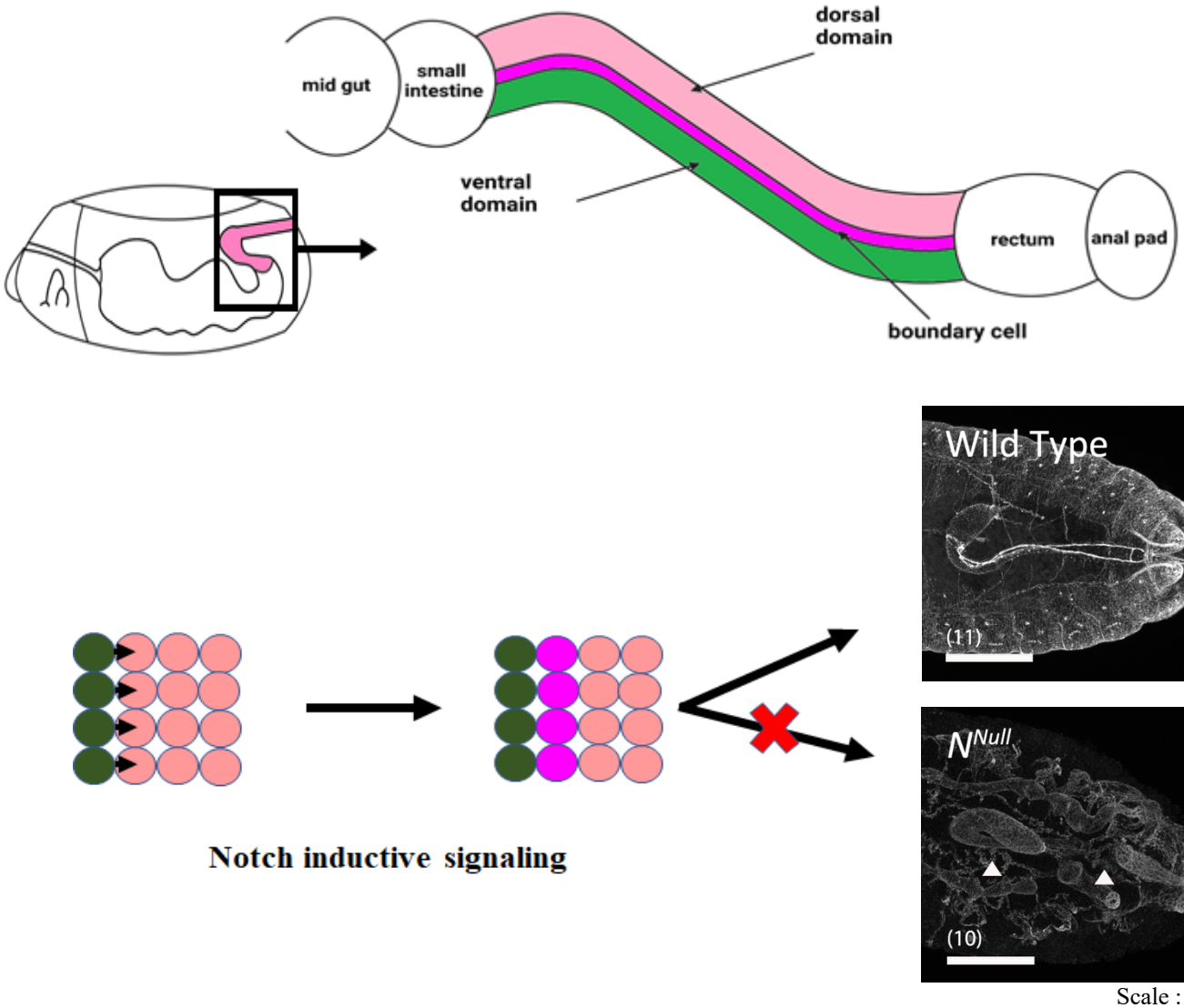

Scale : 50 μm

Figure 10. Notch inductive signaling induces the boundary cells in the embryonic hindgut

Top:

A schematic diagram showing the architecture of embryonic hindgut. The embryonic hindgut is composed of several distinct regions, including the small intestine, large

intestine, and rectum. The large intestine consists of the ventral (green color) and dorsal (cream color) compartments where *Delta* and *engrailed* are expressed, respectively. *Delta* activates Notch signaling is activated within the single row of dorsal cells that consequently differentiate into the boundary cells (magenta color).

Bottom:

Delta-expressing cells are shown in green. The formation of the boundary cells (magenta) is a typical example of inductive Notch signaling (black arrows). In wild type (upper right), the boundary cells highly express *crumbs* and can be detected by an anti-Crumbs antibody staining (white color). However, in loss-of-function mutant of *Notch* (N^{null}, lower right), *crumbs* expression was depleted (shown in white arrowheads), indicating the boundary cells were diminished.

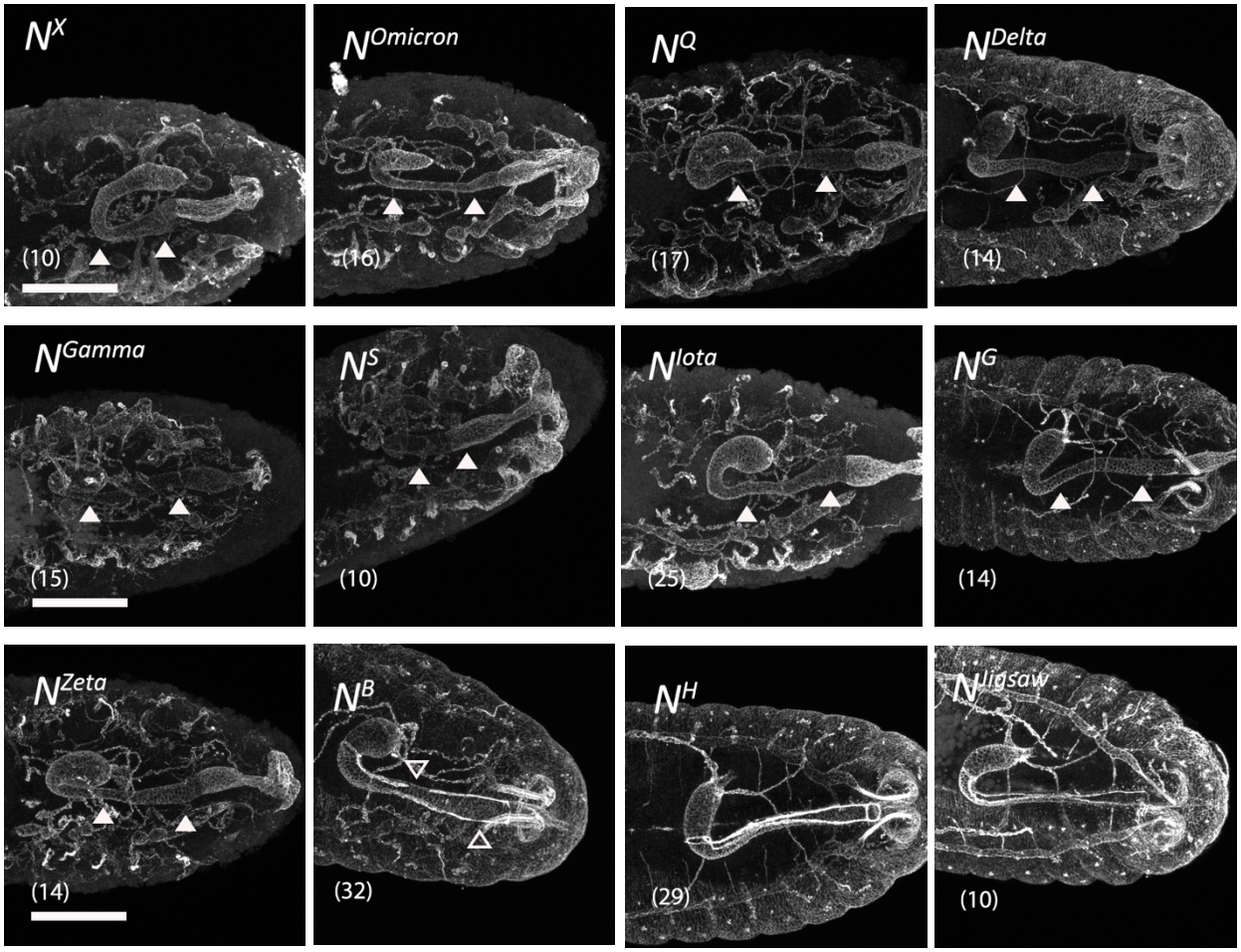

Scale : 50 μm

Figure 11. 10 out of 19 *Notch* mutant alleles showed defects in the formation of the boundary cells

The boundary cells in the embryonic hindgut were detected by an anti-Crumbs antibody staining (white). In 10 out of 19 *Notch* mutant alleles, N^{X}, $N^{omicron}$, N^{Q}, N^{Delta}, N^{Gamma}, N^{S}, N^{Iota}, N^{G}, N^{zeta} and N^{B} the expression of *crumbs* was depleted or showing abnormal gaps (indicated by filled white arrowheads for depleted, and outlined white arrowheads for abnormal gaps). However, the rest of *Notch* mutant alleles showed wild-type boundary

cells, for example, as found in N^{jigsaw} and N^{H} mutants. The names of *Notch* mutant alleles are shown in the upper left. Number shows the numbers of embryos analyzed.

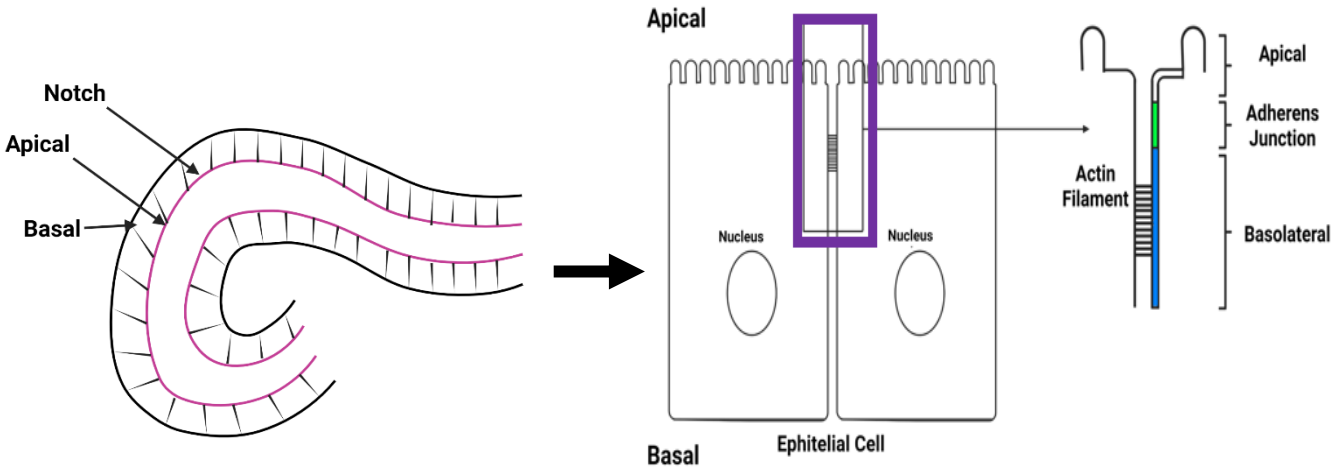

Cross section of the *Drosophila* hindgut epithelium (left), and the localization of Notch protein in the adherens junction of epithelial tissues (right)

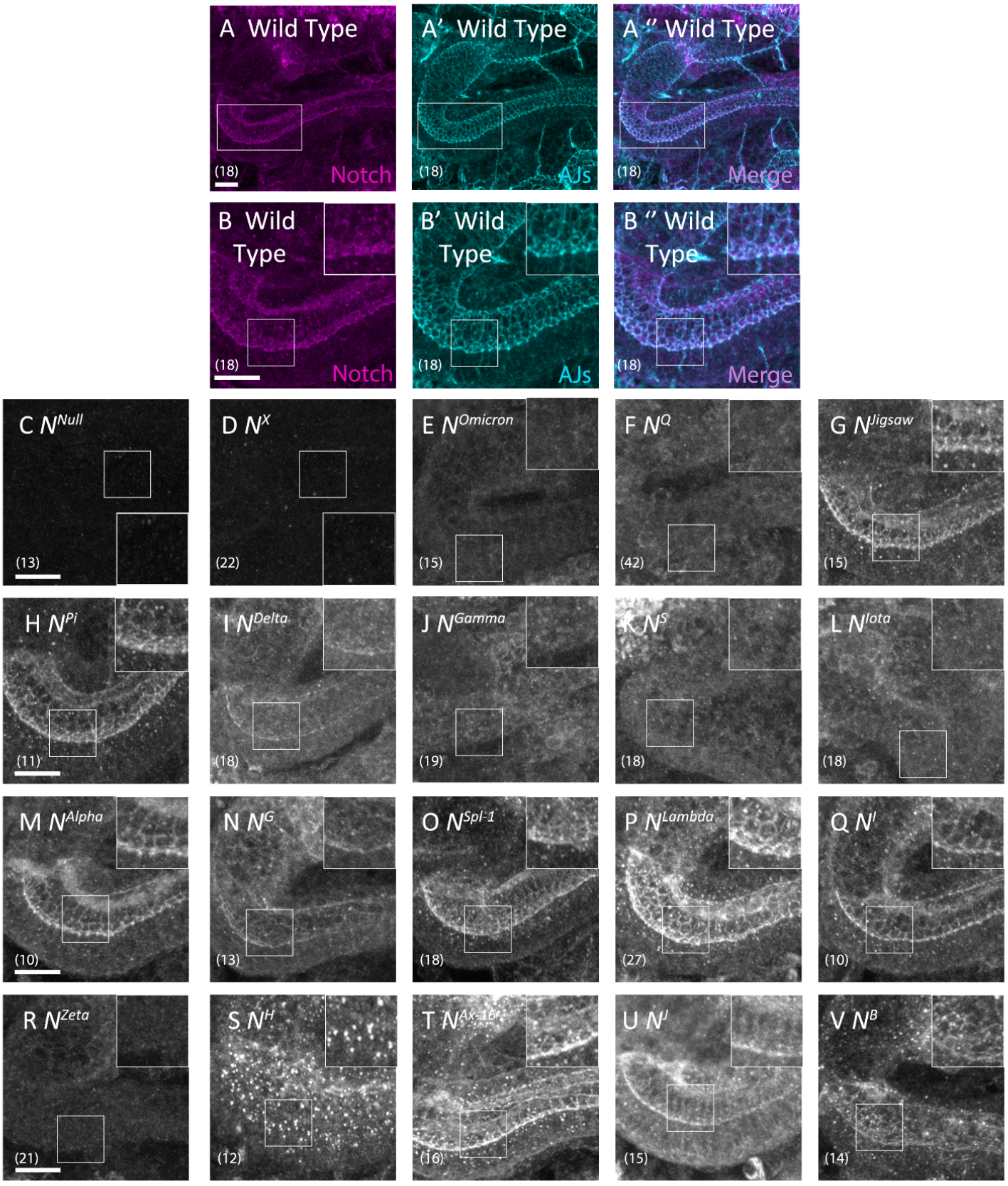
A Wild Type
(18)
Notch
A' Wild Type
(18)
AJs
A '' Wild Type
(18)
Merge
B Wild Type
(18)
Notch
B' Wild Type
(18)
AJs
B '' Wild Type
(18)
Merge
C N^Null
(13)
D N^X
(22)
E N^Omicron
(15)
F N^Q
(42)
G N^Jigsaw
(15)
H N^Pi
(11)
I N^Delta
(18)
J N^Gamma
(19)
K N^S
(18)
L N^Iota
(18)
M N^Alpha
(10)
N N^G
(13)
O N^Spl-1
(18)
P N^Lambda
(27)
Q N^I
(10)
R N^Zeta
(21)
S N^H
(12)
T N^Ax-16
(16)
U N^J
(15)
V N^B
(14)

Scale : 10 µm

Figure 12. 8 out of 19 *Notch* mutant alleles showed abnormal localization of Notch in the hindgut epithelium

Top:

A schematic diagram showing a cross section of the embryonic hindgut is showed.

Bottom:

Notch alleles that disrupted intracellular Notch trafficking. (A, A'' and B, B'') Notch and E-cadherin, a marker of adherens junctions (AJs), were detected in wild-type hindgut epithelium by anti-Notch (magenta in A, B) and anti-E-cadherin (turquoise in A', B') antibody staining. (B, B', B'') show high-magnification views of the regions outlined in (A, A', A''), respectively. Panels (A'', B'') are merged images of panels (A, A', B, B'), respectively. (C-V) Notch was detected by anti-Notch antibody staining (white) in the hindgut epithelium of (C) N^{55e11}, an amorphic allele of *Notch*; (D) N^{X}, (E) $N^{Omicron}$, (F) N^{Q}, (G) N^{Jigsaw}, (H) N^{Pi}, (I) N^{Delta}, (J) N^{Gamma}, (K) N^{S}, (L) N^{Iota}, (M) N^{Alpha}, (N) N^{G}, (O) N^{Spl-1}, (P) N^{Lambda}, (Q) N^{I}, (R) N^{Zeta}, (S) N^{H}, (T) N^{Ax-16}, (U) N^{J}, and (V) N^{B} hemizygotes. Insets are highly magnified images of regions outlined by white rectangles. The number of hindgut samples analyzed is shown in parentheses. Scale bars: 10 μm.

No	Name	EGF-like Repeat	Mutation Position	Notch Trafficking	Notch Localization
1	N^{X}	EGF 8	C343S (C_2S)	Abnormal	Loss
2	$N^{Omicron}$	EGF 8	C343Y (C_2Y)	Abnormal	ER
3	N^{Q}	EGF 8	D331N	Abnormal	ER
4	N^{Jigsaw}	EGF 8	V361M	Normal	AJs
5	N^{Pi}	EGF 9	D374G	Normal	AJs
6	N^{Delta}	EGF 9	D389N	Normal	AJs
7	N^{Gamma}	EGF 9	C398Y (C_5Y)	Abnormal	ER
8	N^{S}	EGF 9	C407S (C_6S)	Abnormal	ER
9	N^{Iota}	EGF 10	C413S (C_1S)	Abnormal	ER
10	N^{Alpha}	EGF 11	E452K	Normal	AJs
11	N^{G}	EGF 13	C535S (C_2S)	Normal	AJs
12	N^{Spl-1}	EGF 14	I578T	Normal	AJs
13	N^{Lambda}	EGF 16	G668R	Normal	AJs
14	N^{I}	EGF 16	G671D	Normal	AJs
15	N^{Zeta}	EGF 25	C993S (C_2S)	Abnormal	ER
16	N^{H}	EGF 29	C1155S (C_2S)	Abnormal	Early endosomes
17	N^{Ax-16}	EGF 29	G1174A	Normal	AJs
18	N^{J}	EGF 34	C1341Y(C_1Y)	Normal	AJs
19	N^{B}	TMD	I1751K	Normal	AJs

Table 2. Results from Notch trafficking analyses and localization are summarized

19 *Notch* mutant alleles examined for the Notch trafficking analyses. All mutants which carry single amino acid mutations in the EGF-like repeats (1-18) or the transmembrane domain (19) are listed in the column of "Name" (Yamamoto, et al., 2012). The positions of EGF-like repeats with amino acid substitutions are shown as the numbers of the EGF-

like repeats from the N-terminal in the column of “EGF like repeat”. The nature of amino acid substitutions is shown in the column of “Mutation position”. Notch trafficking analyzed based on Notch localization are shown. “Normal” indicates Notch located at the AJs, “Abnormal” indicates Notch expression were missing from AJs. Notch localization analyzed were based on the co-localization between Notch and cell compartment markers. “Loss” indicates the missing of Notch expression, “ER” indicates endoplasmic reticulum, and “AJs” indicates adherens junction.

Classes	*Notch* Activity in Neuron & Boundary Cell	Notch Trafficking	*Notch* Alleles
I	Normal	Normal	N^{Jigsaw}, N^{Pi}, N^{Alpha}, N^{Spl-1}, N^{Lambda}, N^{I}, N^{Ax-16}, N^{J}
II	Normal	Abnormal	N^{H}
III	Abnormal	Normal	N^{Delta}, N^{G}, N^{B}
IV	Abnormal	Abnormal	N^{X}, $N^{Omicron}$, N^{Q}, N^{S}, N^{Gamma}, N^{Iota}, N^{Zeta}

Table 3. 19 *Notch* mutant alleles were classified into 4 classes based on the *Notch* activity and trafficking

From the experiment results, I divided mutants into four clusters, each of which based on the phenotypes of the Notch activities in lateral inhibition (Neuron development) and inductive signaling (Boundary cell formation), combined by the data from Notch trafficking. Class I mutant comprises of 8 *Notch* alleles which did not have abnormalities in the *Notch* activities and Notch trafficking. Class II mutant comprises of one *Notch* allele which showed normal *Notch* activities and abnormal Notch trafficking. Class III mutants comprises of 3 *Notch* alleles which showed abnormal *Notch* activities and normal Notch trafficking. Class IV comprises of 7 *Notch* alleles which showed abnormal *Notch* activities and also abnormal Notch trafficking

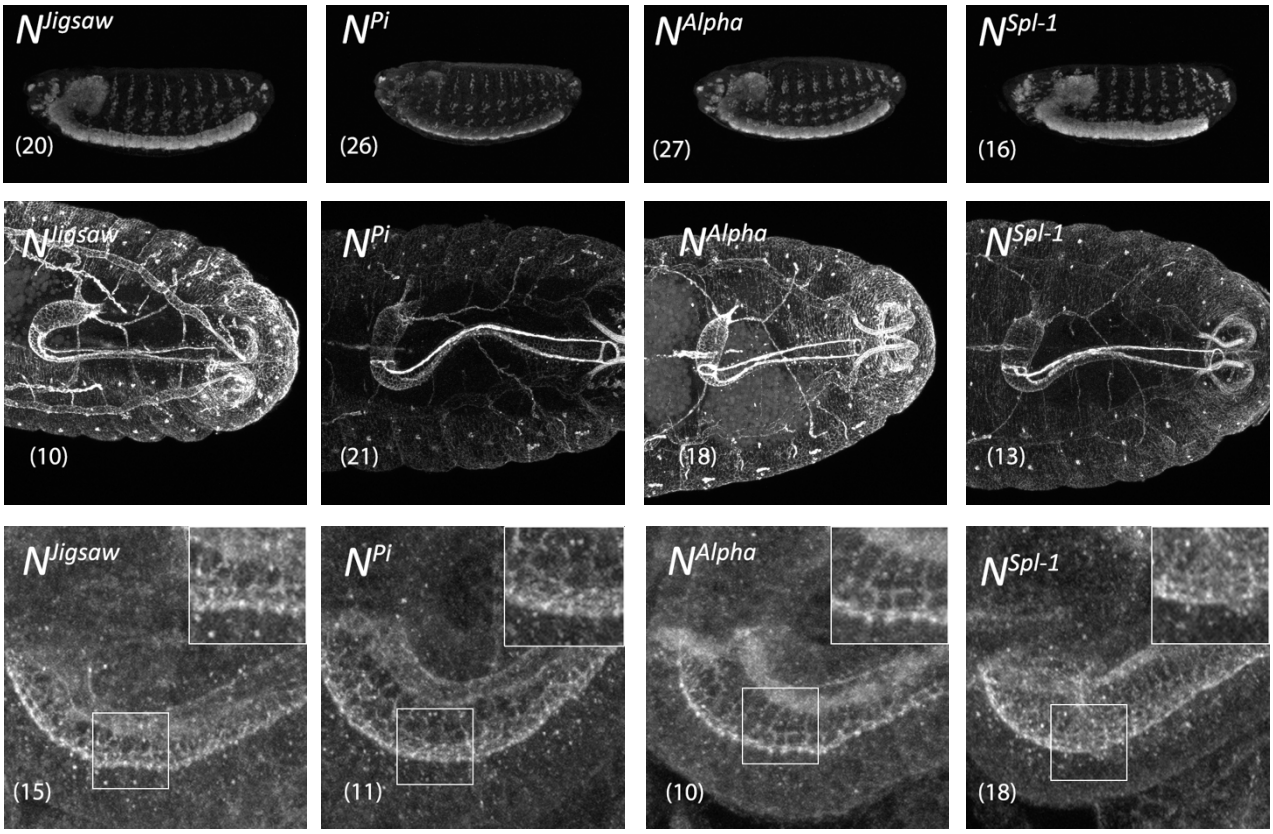
N Jigsaw
(20)
N Pi
(26)
N Alpha
(27)
N Spl-1
(16)
N Jigsaw
(10)
N Pi
(21)
N Alpha
(18)
N Spl-1
(13)
N Jigsaw
(15)
N Pi
(11)
N Alpha
(10)
N Spl-1
(18)

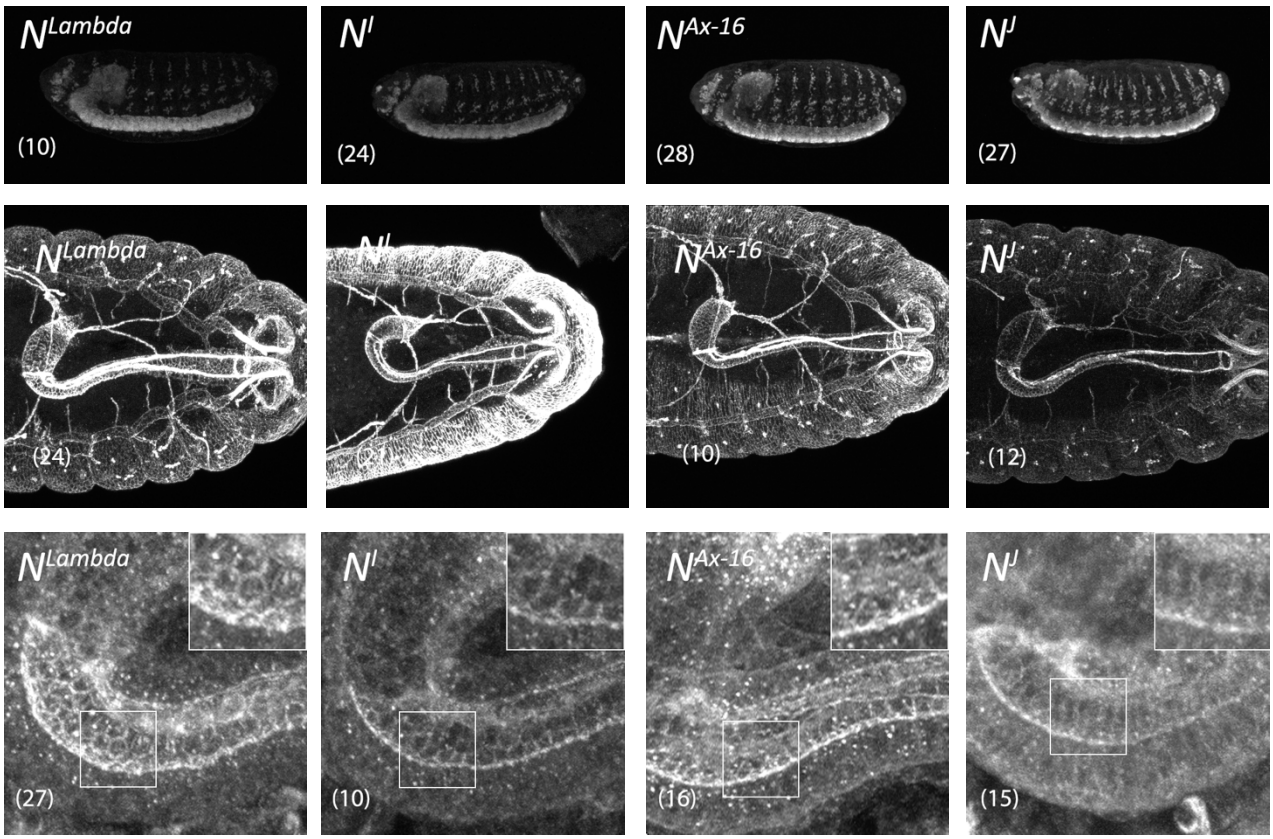
N Lambda
(10)
N l
(24)
N Ax-16
(28)
N J
(27)
N Lambda
(24)
N Ax-16
(10)
N J
(12)
N Lambda
(27)
N l
(10)
N Ax-16
(16)
N J
(15)

Figure 13. Class I mutants showed normal *Notch* activity and trafficking

These are eight mutants which clustered into the class I. This class consist of N^{Jigsaw}, N^{Pi} , N^{Alpha}, N^{Spl-1}, N^{Lambda}, N^{I}, N^{Ax-16}, and N^{J}, All of which showed to have normal *Notch* activities (lateral inhibition and inducive signaling) and normal Notch trafficking. The mutants are shown in two rows, each of which consist of 4 mutants and showed in 3 parameters. The first parameter (top panel) is *Notch* activity in lateral inhibition showed by the nervous system, shown in white. Second parameter (center panel) is *Notch* activity in inductive signaling showed by boundary cells in white. Third parameter (lower panel) is Notch trafficking shown in white. Insets are highly magnified images of regions outlined by white rectangles. The names of *Notch* mutant alleles are shown in the upper left. Number shows the numbers of embryos analyzed. The same rules also apply in the second row of the mutants

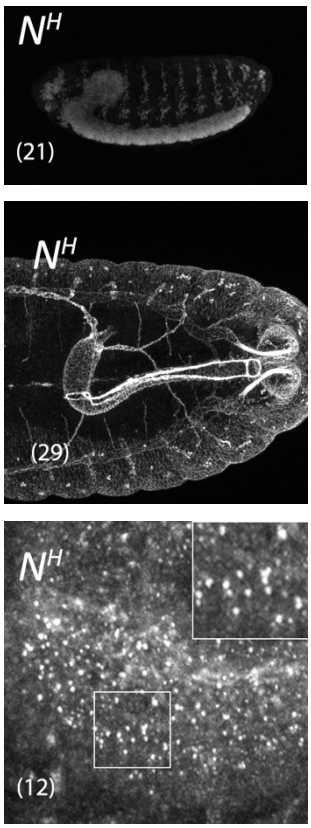

Figure 14. Class II mutant showed normal *Notch* activity, but its trafficking was abnormal

Class II mutant consist of one *Notch* mutant, N^H. This mutant showed to have normal *Notch* activities in both of lateral inhibition (top panel, nervous system shown in white) and inductive signaling (center panel, boundary cells shown in white). However, this mutant showed to have abnormal Notch trafficking (lower panel, Notch showed in white). Inset are highly magnified image of region outlined by white rectangle. The name of *Notch* mutant allele is shown in the upper left. Number shows the numbers of embryos analyzed.

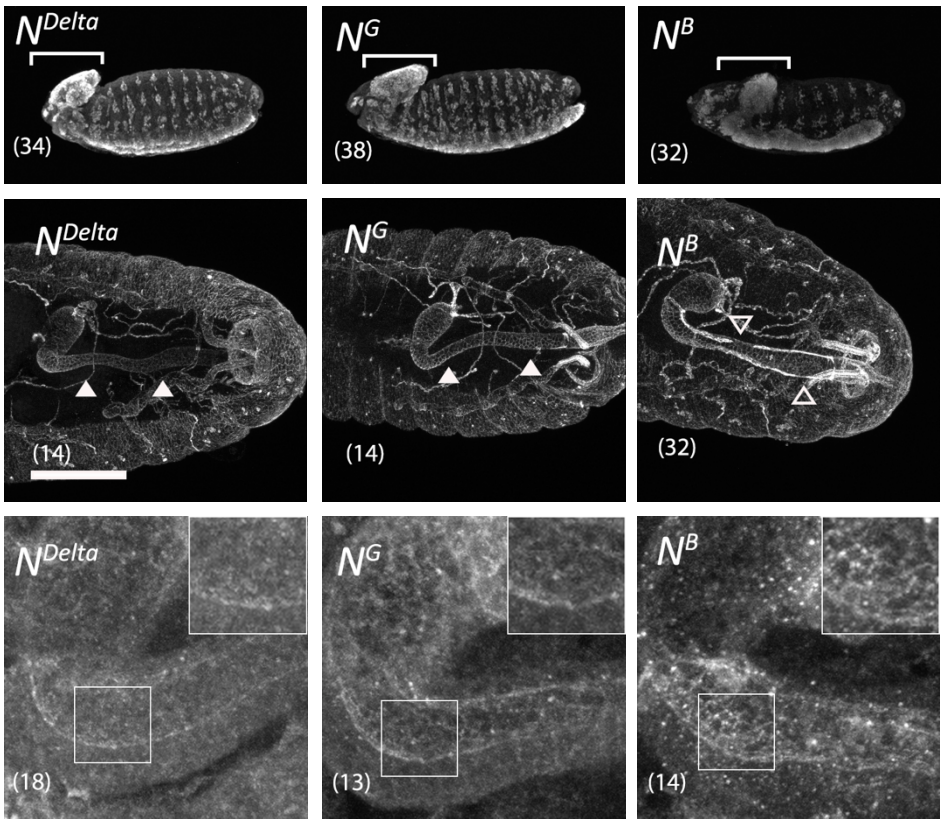

Figure 15. Class III mutants showed abnormal *Notch* activity, but its trafficking was normal

Class III mutants consist of N^{Delta}, N^{G} *and* N^{B}, and showed to have loss or reduced of *Notch* activities in the lateral inhibition (top panel, brain defromation showen by white brackets) and inductive signaling (center panel boundary cells showed in white). However, normal or insignificant disruption were observed in the Notch trafficking (lower panel, Notch showed in white). The names of *Notch* mutant alleles are shown in the upper left. Number shows the numbers of embryos analyzed. White brackets in the top panel showed brain deformation. Filled white arrowheads in central panels showed depletion in

boundary cells, while outlined white arrowheads showed abnormal gaps in boundary cells, respectively. Insets in the lower panel are highly magnified images of regions outlined by white rectangles.

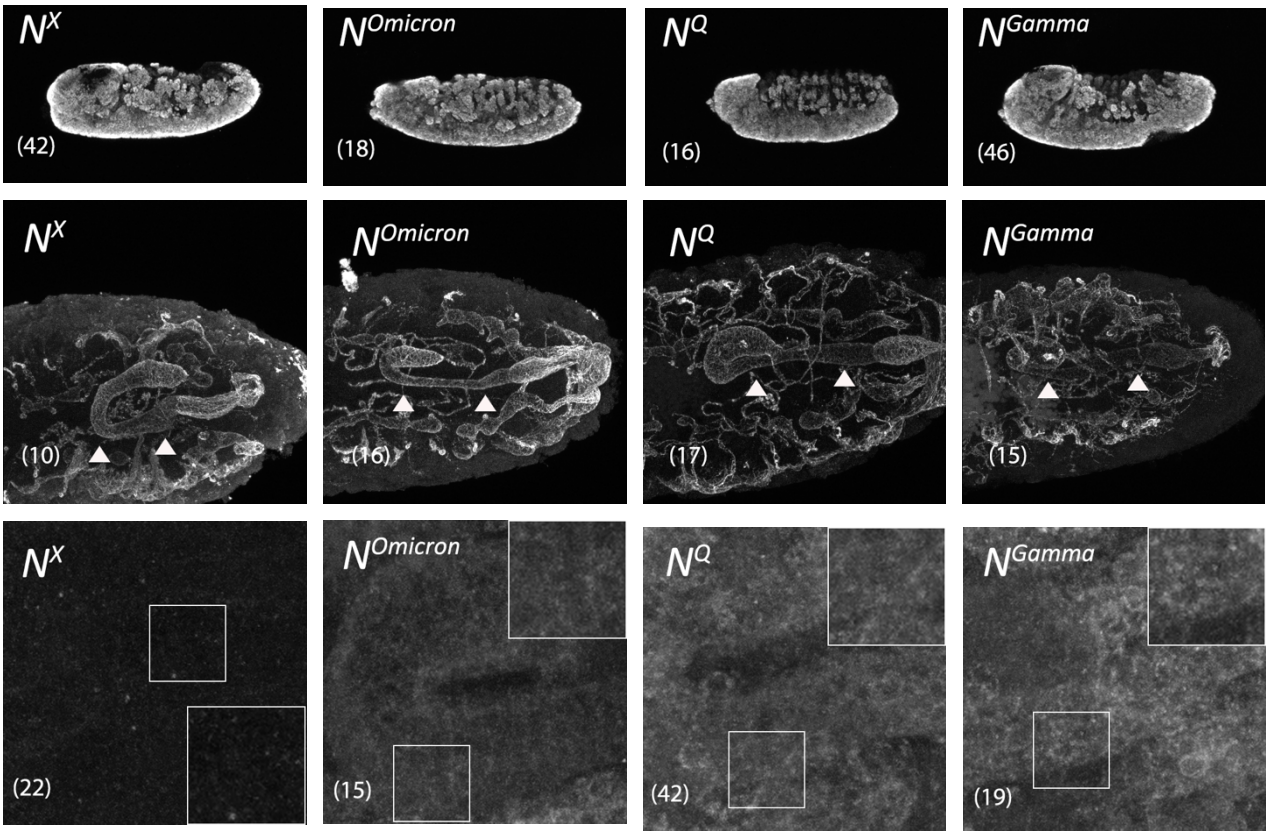

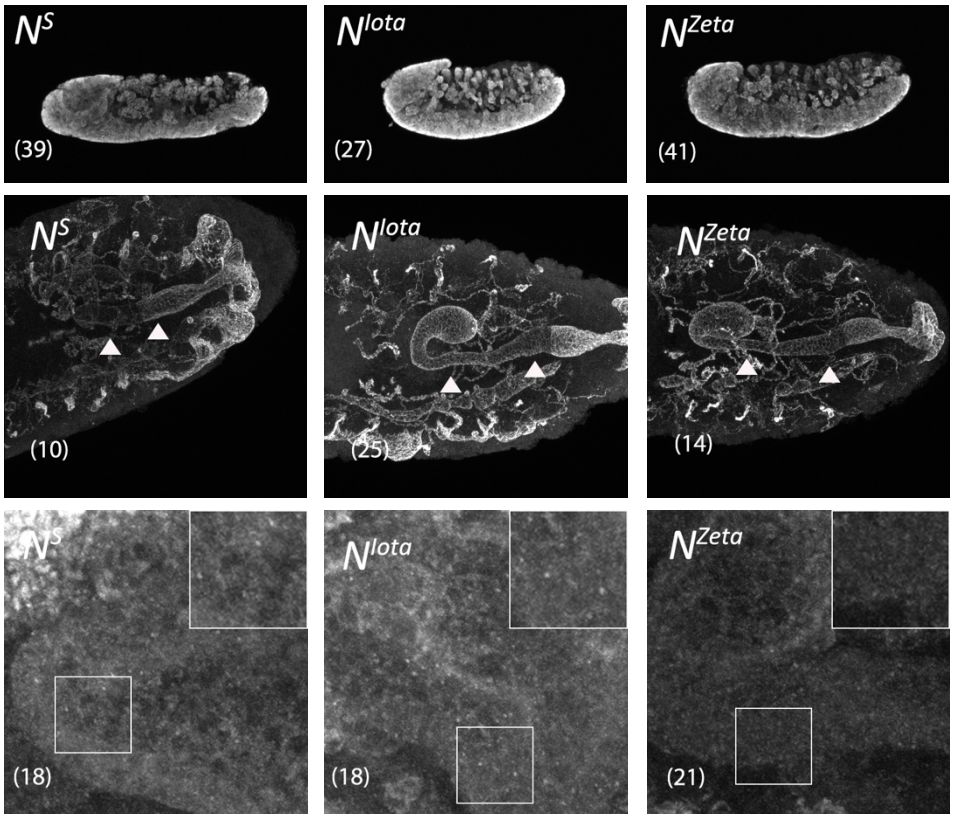

Figure 16. Class IV mutants showed loss of *Notch* activity and abnormal Notch trafficking

Class IV mutants consist of 7 mutants which showed to have abnormal *Notch* activity and trafficking. The mutants are N^{X}, $N^{Omicron}$, N^{Q}, N^{Gamma}, N^{S}, N^{Iota} *and* N^{Zeta} , all of which showed loss of Notch activity in the central nervous system and boundary cells, as well as in Notch trafficking. The mutants showed in two rows, each of which consist of 4 mutants and 3 mutants, respectively. Each row showed in 3 different parameters. The first parameter (top panel) is *Notch* activity in lateral inhibition showed by the nervous system

in white. Second parameter (center panel) is the *Notch* activity in inductive signaling showed by boundary cells in white. Third parameter (lower panel) is Notch trafficking, showed in white. The names of *Notch* mutant alleles are shown in the upper left. Number shows the numbers of embryos analyzed. White arrowhead showed abnormal boundary cell formation in the center panel. Insets in the lower panel are highly magnified images of regions outlined by white rectangles. The same rules also apply in the second row of the mutants.

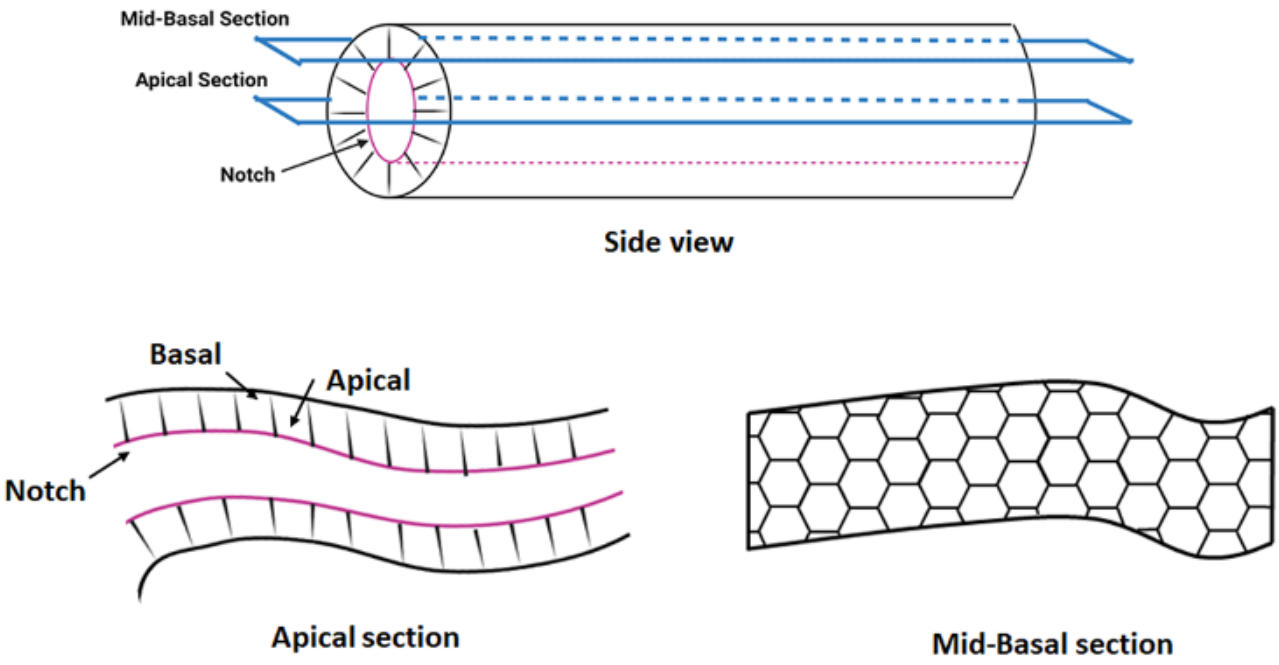

Sections of *Drosophila* hindgut

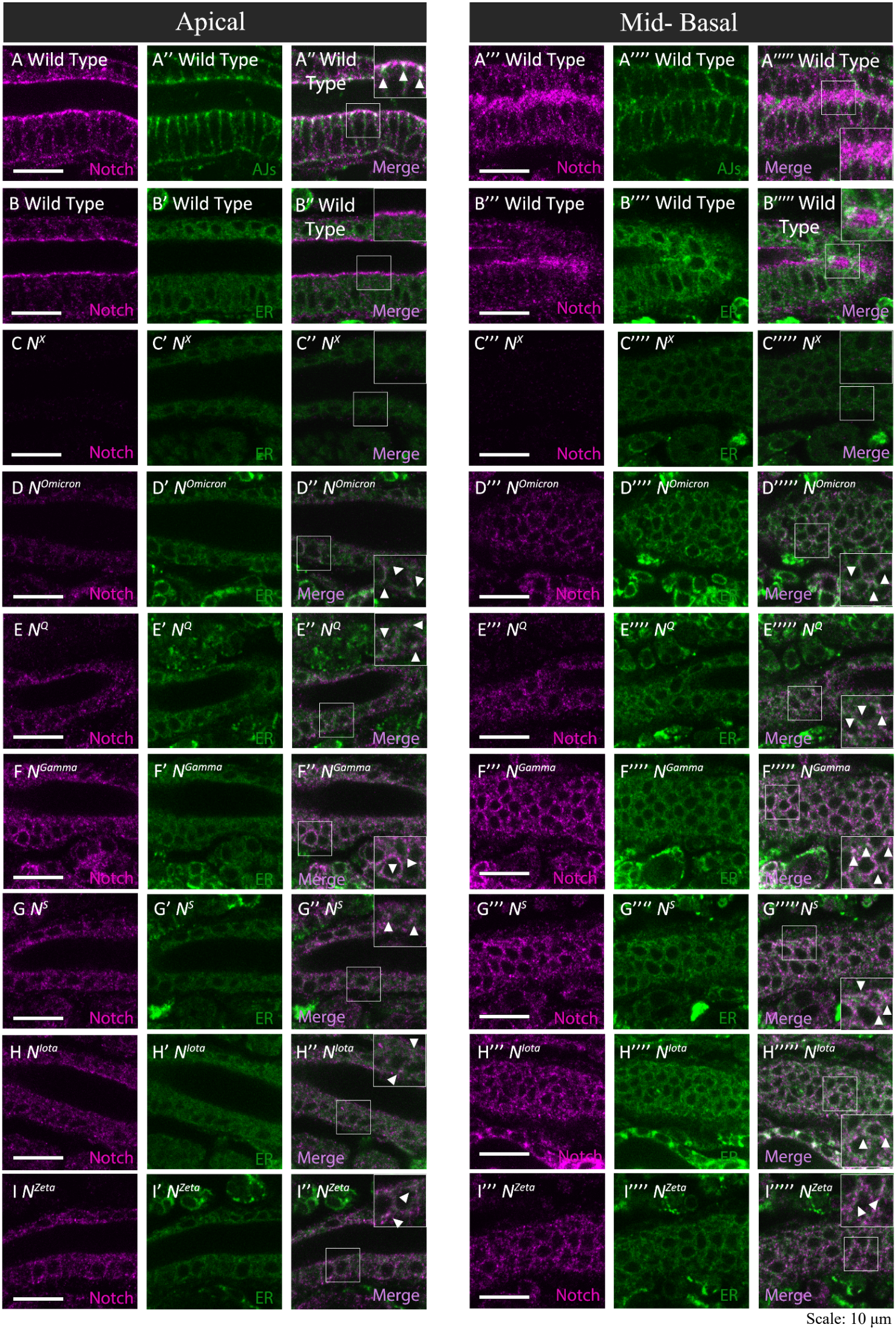
Apical
Mid- Basal
A Wild Type
A'' Wild Type
A'' Wild Type
A''' Wild Type
A'''' Wild Type
A''''' Wild Type
B Wild Type
B' Wild Type
B'' Wild Type
B''' Wild Type
B'''' Wild Type
B''''' Wild Type
C N^X
C' N^X
C'' N^X
C''' N^X
C'''' N^X
C''''' N^X
D $N^{Omicron}$
D' $N^{Omicron}$
D'' $N^{Omicron}$
D''' $N^{Omicron}$
D'''' $N^{Omicron}$
D''''' $N^{Omicron}$
E N^Q
E' N^Q
E'' N^Q
E''' N^Q
E'''' N^Q
E''''' N^Q
F N^{Gamma}
F' N^{Gamma}
F'' N^{Gamma}
F''' N^{Gamma}
F'''' N^{Gamma}
F''''' N^{Gamma}
G N^S
G' N^S
G'' N^S
G''' N^S
G'''' N^S
G''''' N^S
H N^{Iota}
H' N^{Iota}
H'' N^{Iota}
H''' N^{Iota}
H'''' N^{Iota}
H''''' N^{Iota}
I N^{Zeta}
I' N^{Zeta}
I'' N^{Zeta}
I''' N^{Zeta}
I'''' N^{Zeta}
I''''' N^{Zeta}
Notch
AJs
ER
Merge

Scale: 10 µm

Figure 17. Schema showing cross sections of *Drosophila* hindgut, and most of Class IV mutants showed colocalization between Notch and ER marker

Top:

A schematic diagram to show cross sections of the hindgut. This observations were taken from half section of the hindgut to observe apical side, followed by mid-basal section.

Bottom:

Notch accumulated abnormally in the ER of the hindgut epithelium in Class IV *Notch* mutants. (A-I’’’’’) Apical and mid-basal images corresponding to the diagrams of apical and mid-basal planes. (A-B’’’’’) Wild-type hindgut epithelium stained for Notch (magenta in A, A’’, A’’’, A’’’’’, B, B’’, B’’’, B’’’’’), E-Cadherin (green in A’, A’’, A’’’, A’’’’’), and the ER marker Pdi-GFP (green in B’,B’’,B’’’’,B’’’’’) using anti-Notch, anti-E-Cadherin, and anti-GFP antibodies. (C-I’’’’’) Notch (magenta, left panels) and Pdi-GFP (green, middle panels) were observed by anti-Notch and anti-GFP antibody staining, respectively, in the hindgut epithelium of (C-C’’’’’) N^{X}, (D-D’’’’’) $N^{Omicron}$, (E-E’’’’’) N^{Q}, (F-F’’’’’) N^{Gamma}, (G-G’’’’’) N^{S}, (H-H’’’’’) N^{iota}, and (I-I’’’’’) N^{Zeta} hemizygotes. Right-side panels in apical and mid-basal images, indicated by ’’ and ’’’’’, respectively, are merged from the left and middle images. Insets in the right panels indicated by ’’ and ’’’’’ are highly magnified views of regions in white rectangles. Intracellular punctae where Notch and Pdi-GFP colocalized are shown by white arrowheads.

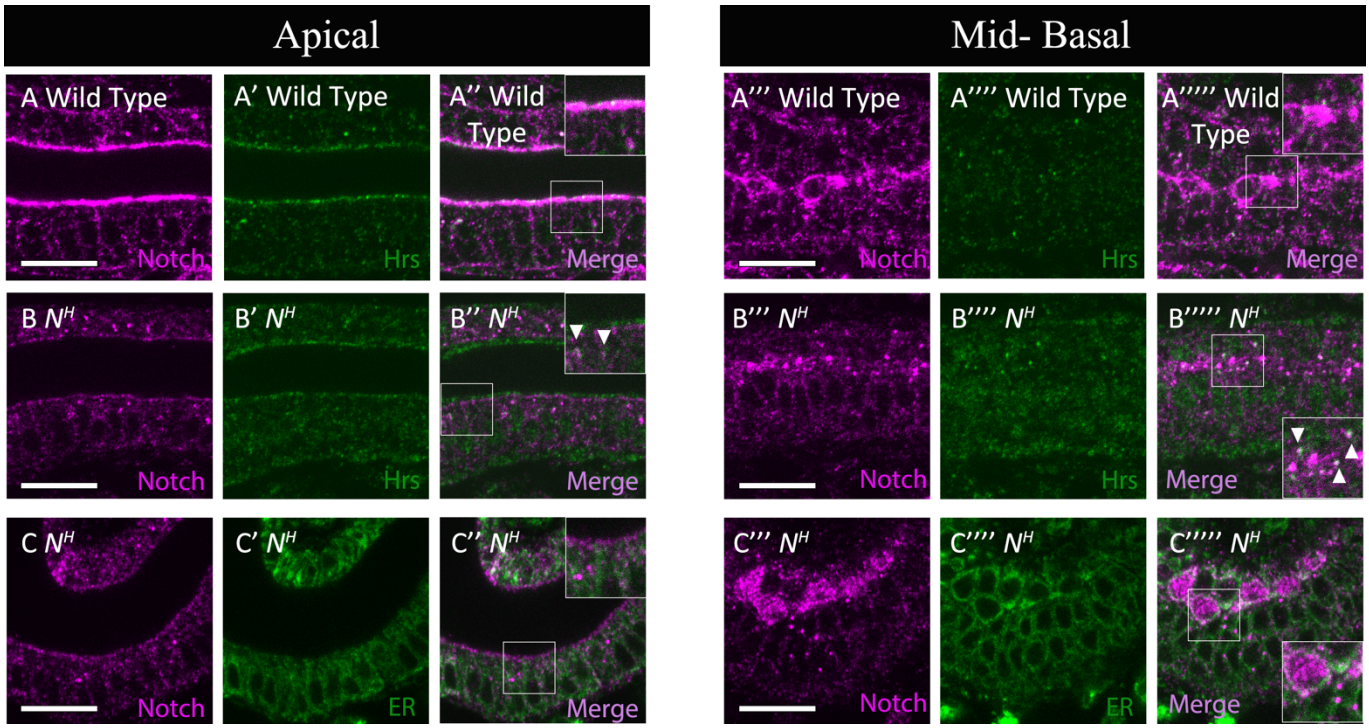

Scale: 10 μm

Figure 18. In Class II mutants, Notch colocalized with Hrs, marker of early endosomes

Notch accumulated abnormally in early endosomes of the hindgut epithelium in a Class II *Notch* mutant. The apical and mid-basal sections correspond to the previous figure 17 and shown in microscopic images in (A-C'') and (A'''-C'''''), respectively, as indicated in the top of (A-C'''''). (A-A''''') In wild-type hindgut epithelium, Notch (magenta) and Hrs (green), a marker of early endosomes, were stained with an anti-Notch (A, A'', A''', A''''') and anti-Hrs antibodies (A', A'', A''', A'''''), respectively. (B-C''''') Hindgut epithelium in the N^H hemizygote, a Class II Notch mutant, stained for Notch (magenta in B, B'',B''', B''''', C, C'', C''', C'''''), Hrs (green in B', B'', B''', B'''''), and Pdi-GFP, an ER marker

(green in C', C'', C''', C''''') were observed by anti-Notch, anti-Hrs, and anti-GFP antibody staining, respectively. Insets in (A'', A''''', B'', B''''', C'', C''''') are highly magnified images of regions outlined by white rectangles. White arrowheads point colocalized expression.

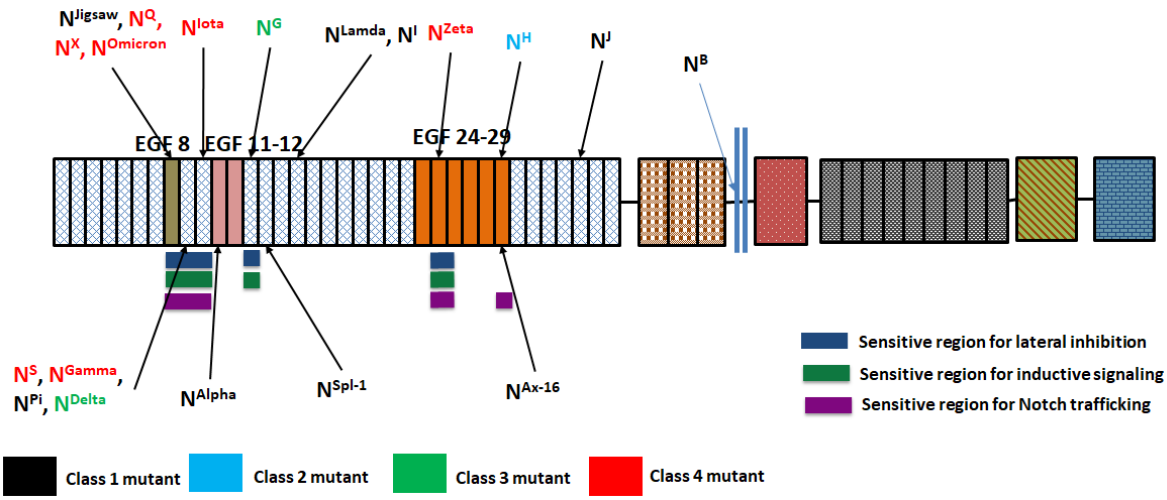

Figure 19. Specific regions of EGF-like repeats which are sensitive to the structural perturbations and affect Notch activity and trafficking

From the experiments, I found that mutations in the particular regions within the EGF-like repeats were sensitive to induce perturbation in the *Notch* activity and trafficking. I found that mutations form clusters in the EGF 8-10 and EGF 25, showed to alter *Notch* activities which resulted in defects of the lateral inhibition and inductive signaling, as well as in Notch trafficking. Blue line shows sensitive region for lateral inhibition, green

line shows sensitive region for inductive signaling, and purple line shows sensitive region for Notch trafficking. In addition to that, these two regions were corresponding with the previously established EGF-8 which plays role in the ligand preference phenomena and in the Abruptex domain in EGF 24-29. Therefore, I suggest that those locations were sensitive regions for the *Notch* activity and trafficking and susceptible to the mutation.

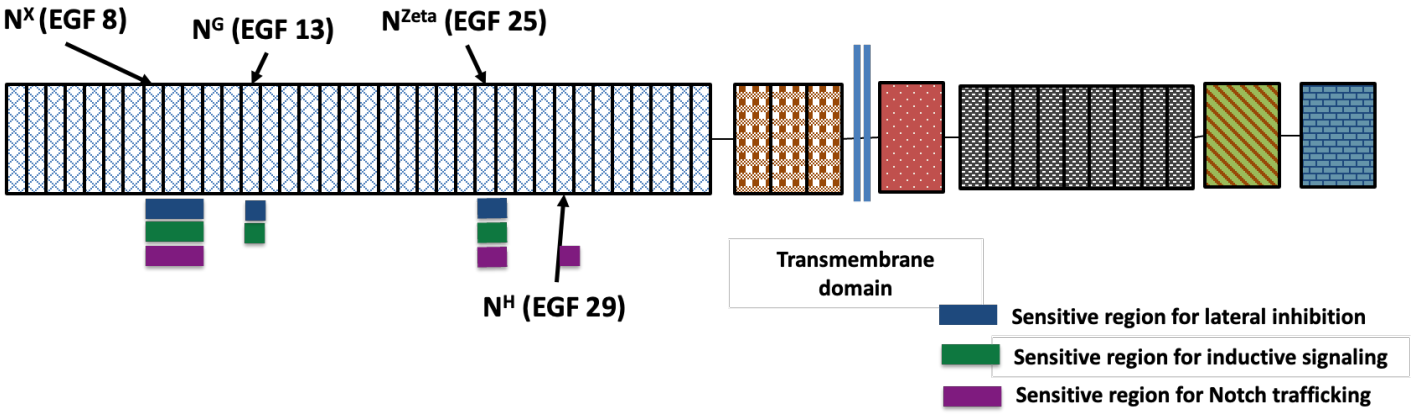

No	Name	EGF–like Repeat	Mutation Position	Notch activity	Notch Trafficking	Notch Localization
1	N^X	EGF 8	C343S (C_2S)	Loss	Abnormal	Loss
2	N^G	EGF 13	C535S (C_2S)	Loss	Normal	Apical/Adherens Junction
3	N^{Zeta}	EGF 25	C993S (C_2S)	Loss	Abnormal	ER
4	N^H	EGF 29	C1155S (C_2S)	Normal	Abnormal	Early Endosome

Figure 20. Mutations inducing the same amino acid substitution (C2S) in different EGF-like repeats give distinct effects on the Notch activity and trafficking

To exclude the possibility that variety of amino acids substituted in each *Notch* mutant allele may affect the interpretation of the results, I compared four *Notch* mutants, which carry same amino acid substitution in the second cysteine to become serine (C2S) in different EGF-like repeats. These four *Notch* mutants are N^{X} (EGF-8, C343S), N^{G} (EGF-13, C535S), N^{Zeta} (EGF-25, C993S) and N^{H} (EGF-29, C1155S). I found that they demonstrated distinct effect on Notch activity and trafficking. More importantly, characteristics of the defects in Notch activity and trafficking observed in these four mutants accord with the cluster of sensitive regions of EGF-like repeats. Therefore, in despite of the limitation in the number of *Notch* alleles used, these analyses provide enough information regarding the specificity of each EGF-like repeats in the activity and folding of Notch.

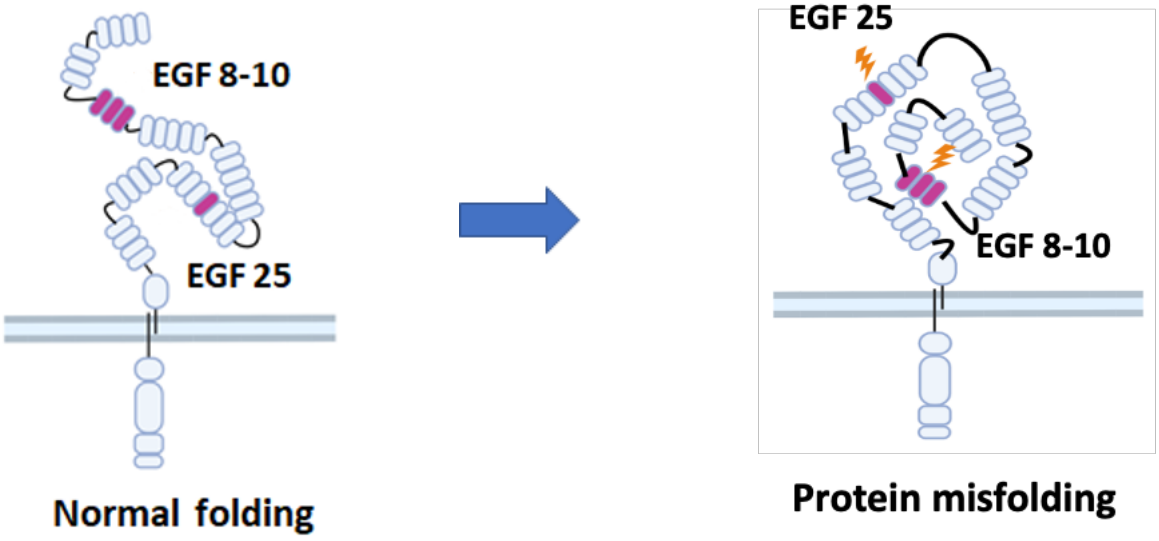

Mutations in the sensitive regions

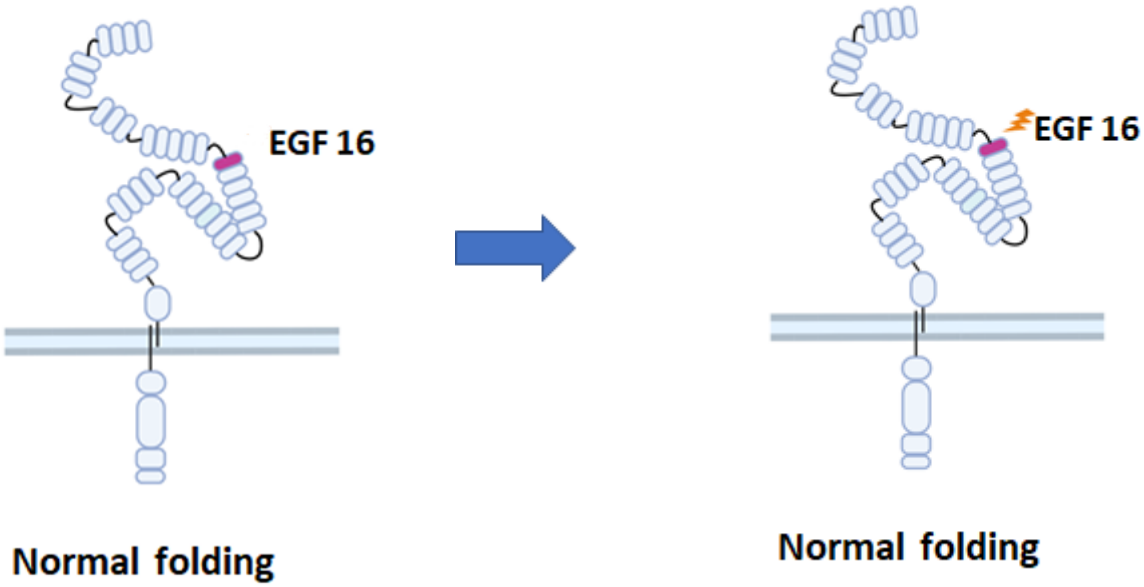

Mutation in the insensitive regions

Figure 21. Models of Notch structure which illustrate EGF 8-10 and EGF 25 as sensitive regions, which are susceptible to the mutations inducing misfolding of Notch

Here, I propose an illustrative model of Notch structure, which highlight specific regions of EGF-like repeats susceptible to structural perturbation. However, this model has not been tested by the approach of structural biology analysis, such as NMR or X-ray. I suggest that EGF-like repeats 8-10 and 25 are particularly impotent to maintain high-order structure of Notch. Therefore, these EGF-like repeats became hotspots which are susceptible to the mutations inducing global misfolding of Notch. This model should provide valuable insights into the future studies to understand the correlation between the structure and function of Notch.

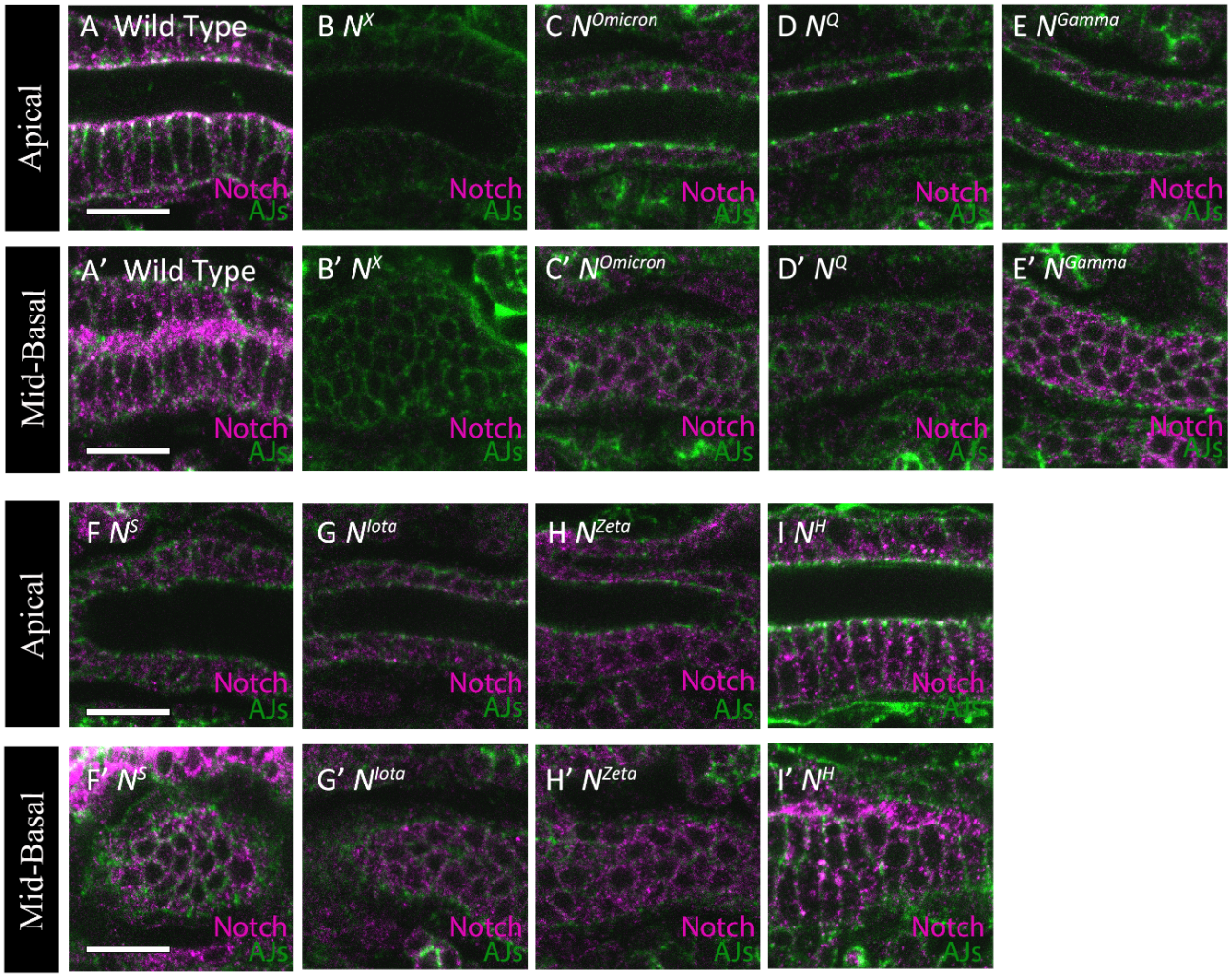

Figure 22. Notch localized to AJs in Class II and IV *Notch* mutants

(A-I') Notch (magenta) and adherens junctions (AJs; green) in hindgut epithelia in wild-type *Drosophila* (A and A') and in hemizygotes of N^X (B and B'), $N^{Omicron}$ (C and C'), N^Q (D and D'), N^{Gamma} (E and E'), N^S (F and F'), N^{Iota} (G and G'), N^{Zeta} (H and H'), and N^H (I and I'), stained by anti-Notch and anti-E-cadherin antibodies, respectively. Apical and mid-basal images (left side) correspond to the diagram of apical and mid-basal planes in Figure 17. Scale bars: 10 μm.

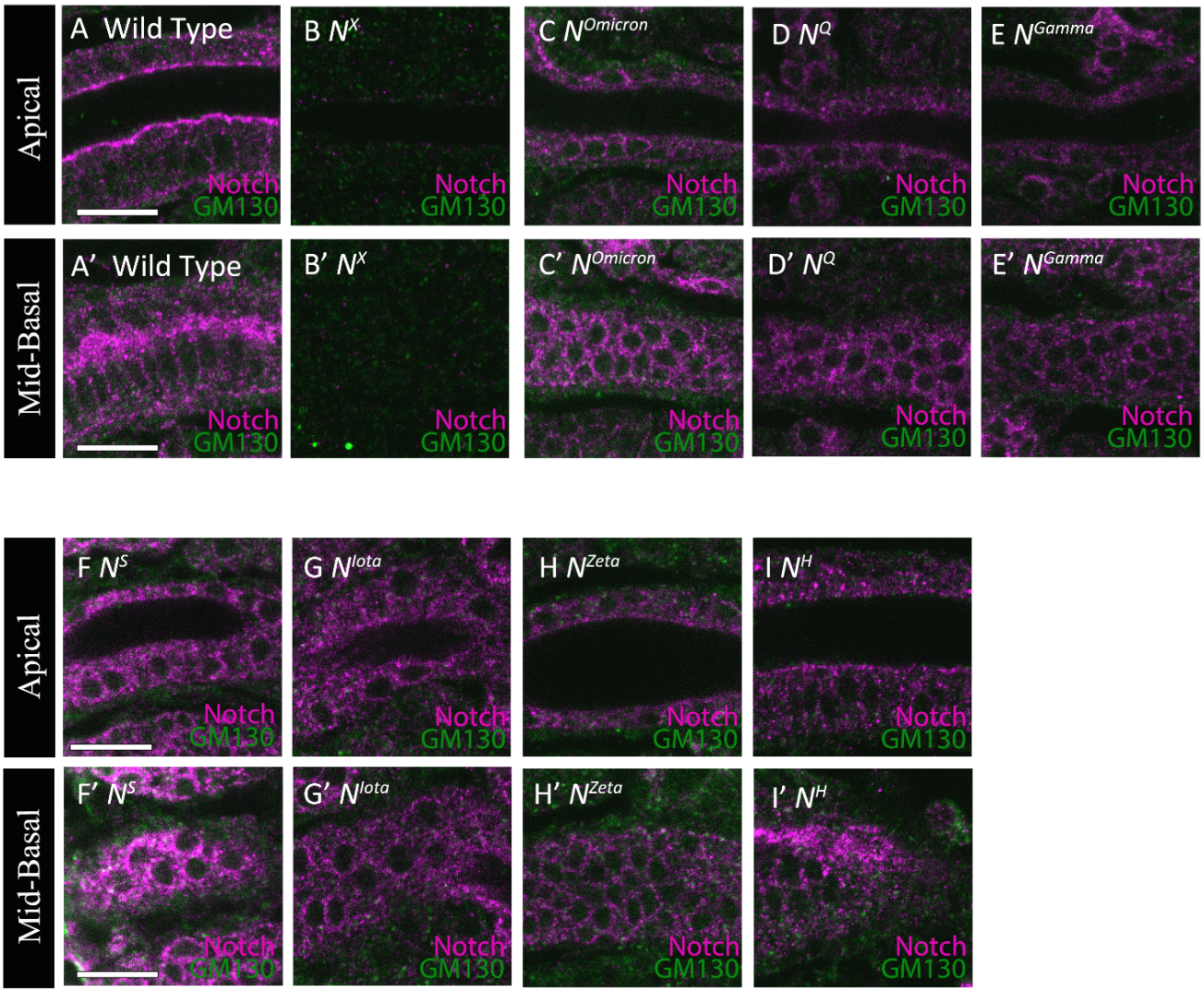

Figure 23. Class II and IV *Notch* mutants did not accumulate Notch in *cis*-Golgi.

(A-I') Notch (magenta) and *cis*-Golgi (green) of hindgut epithelia in wild type (A and A') and hemizygotes of N^X (B and B'), $N^{omicron}$ (C and C'), N^Q (D and D'), N^{Gamma} (E and E'), N^S (F and F'), N^{Iota} (G and G'), N^{Zeta} (H and H'), and N^H (I and I') were detected by anti-Notch and anti-GM130 antibody staining, respectively. Apical and mid-basal images (left

side) correspond to the diagram of apical and mid-basal planes in Figure 17. Scale bars: 10 μm.

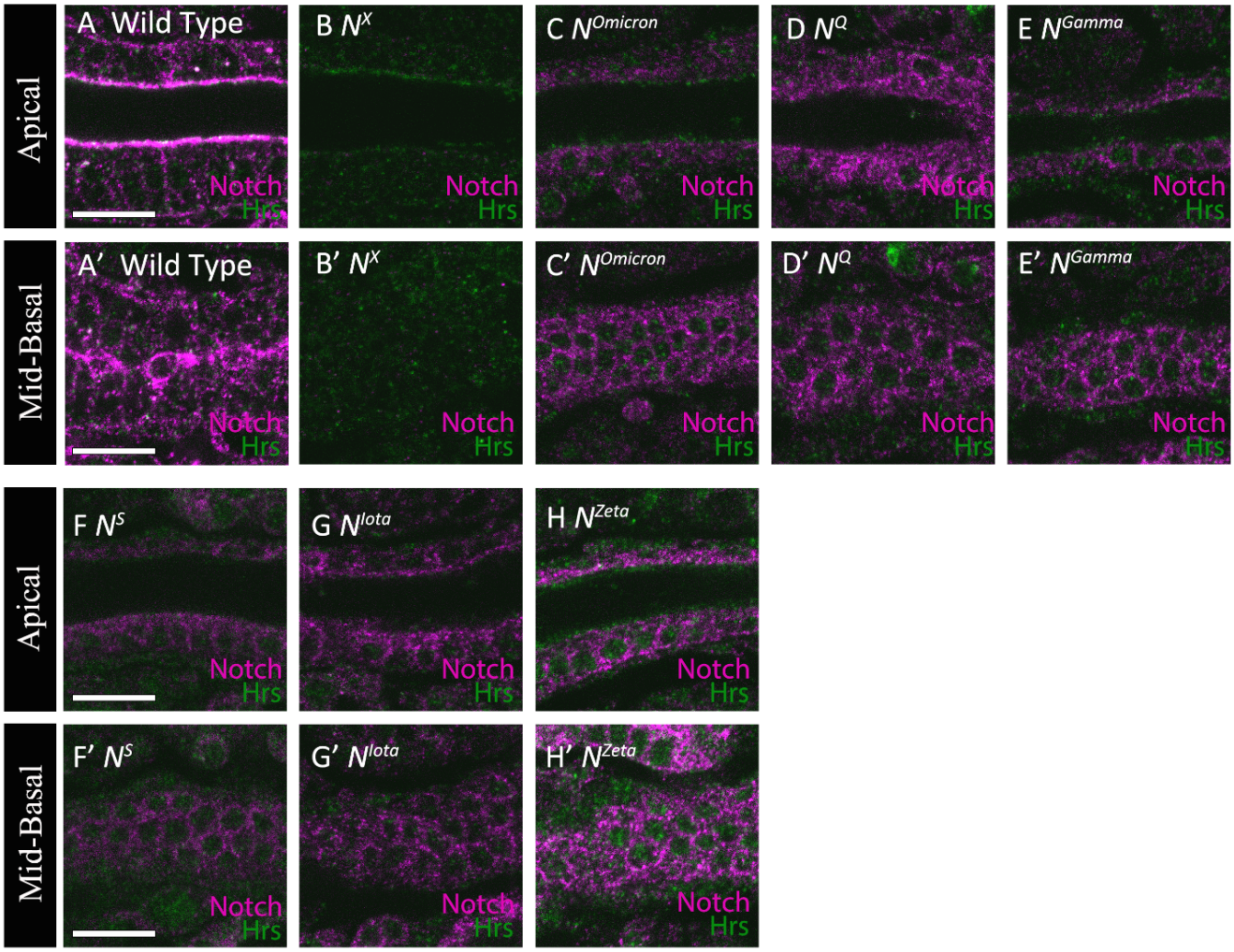

Figure 24. Class IV *Notch* mutants did not accumulate Notch in early endosomes

(A-H') Notch (magenta) and early endosomes (green) of hindgut epithelia in wild type (A and A') and in hemizygotes of N^X (B and B'), $N^{omicron}$ (C and C'), N^Q (D and D'), N^{Gamma} (E and E'), N^S (F and F'), N^{Iota} (G and G'), and N^{Zeta} (H and H') were detected by anti-

Notch and anti-Hrs antibody staining, respectively. Apical and mid-basal images (left side) correspond to the diagram of apical and mid-basal planes in Figure 17. Scale bars: 10 μm

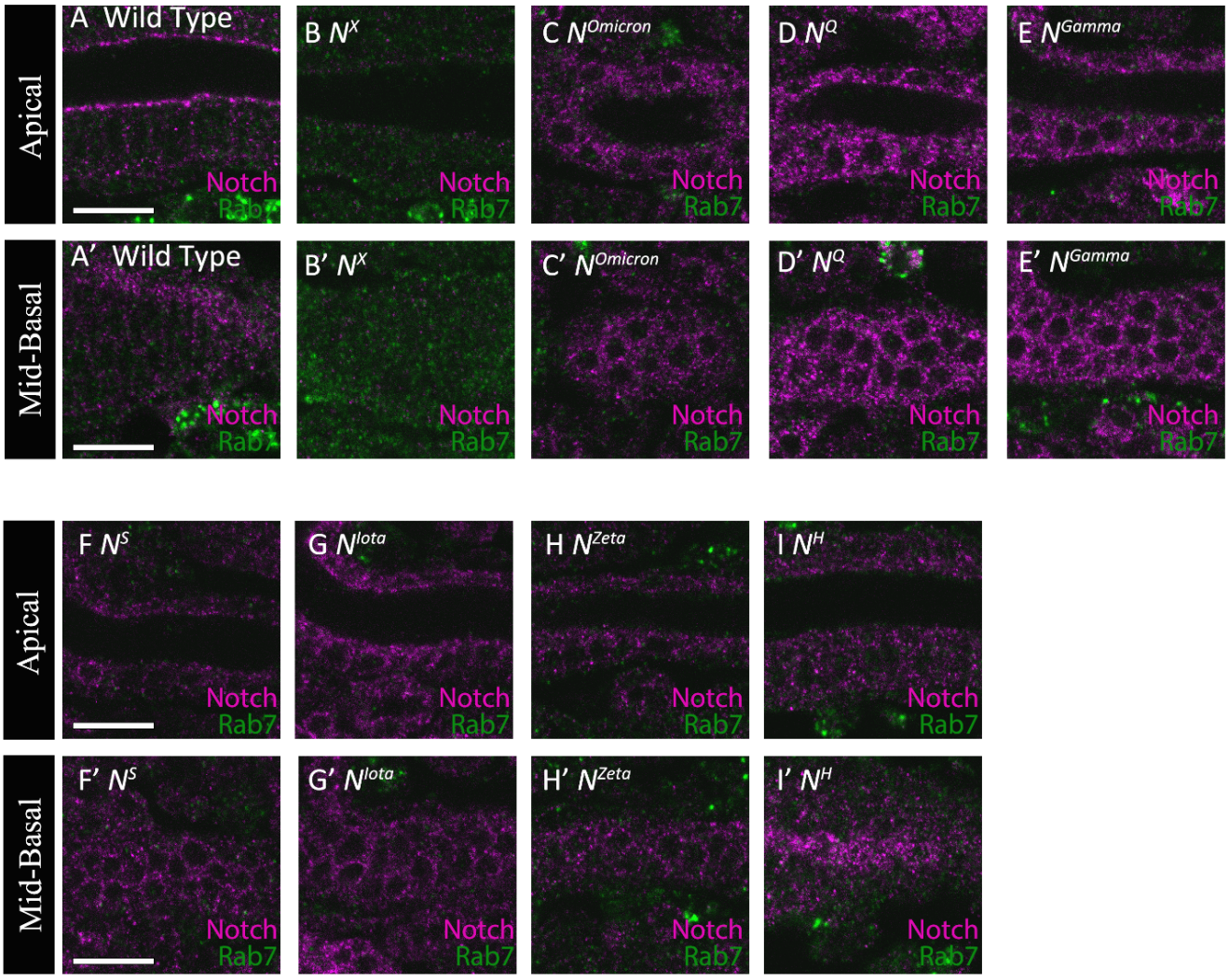

Figure 25. Class II and IV *Notch* mutants did not accumulate Notch in late endosomes

(A-I') Notch (magenta) and late endosomes (green) of hindgut epithelia in wild-type embryos (A and A') and hemizygotes of N^{X} (B and B'), $N^{omicron}$ (C and C'), N^{Q} (D and D'), N^{Gamma} (E and E'), N^{S} (F and F'), N^{Iota} (G and G'), N^{Zeta} (H and H'), and N^{H} (I and I'), detected with anti-Notch and anti-Rab7 antibody staining, respectively. Apical and mid-basal images (left side) correspond to the diagram of apical and mid-basal planes as described in Figure 17. Scale bars: 10 μm.

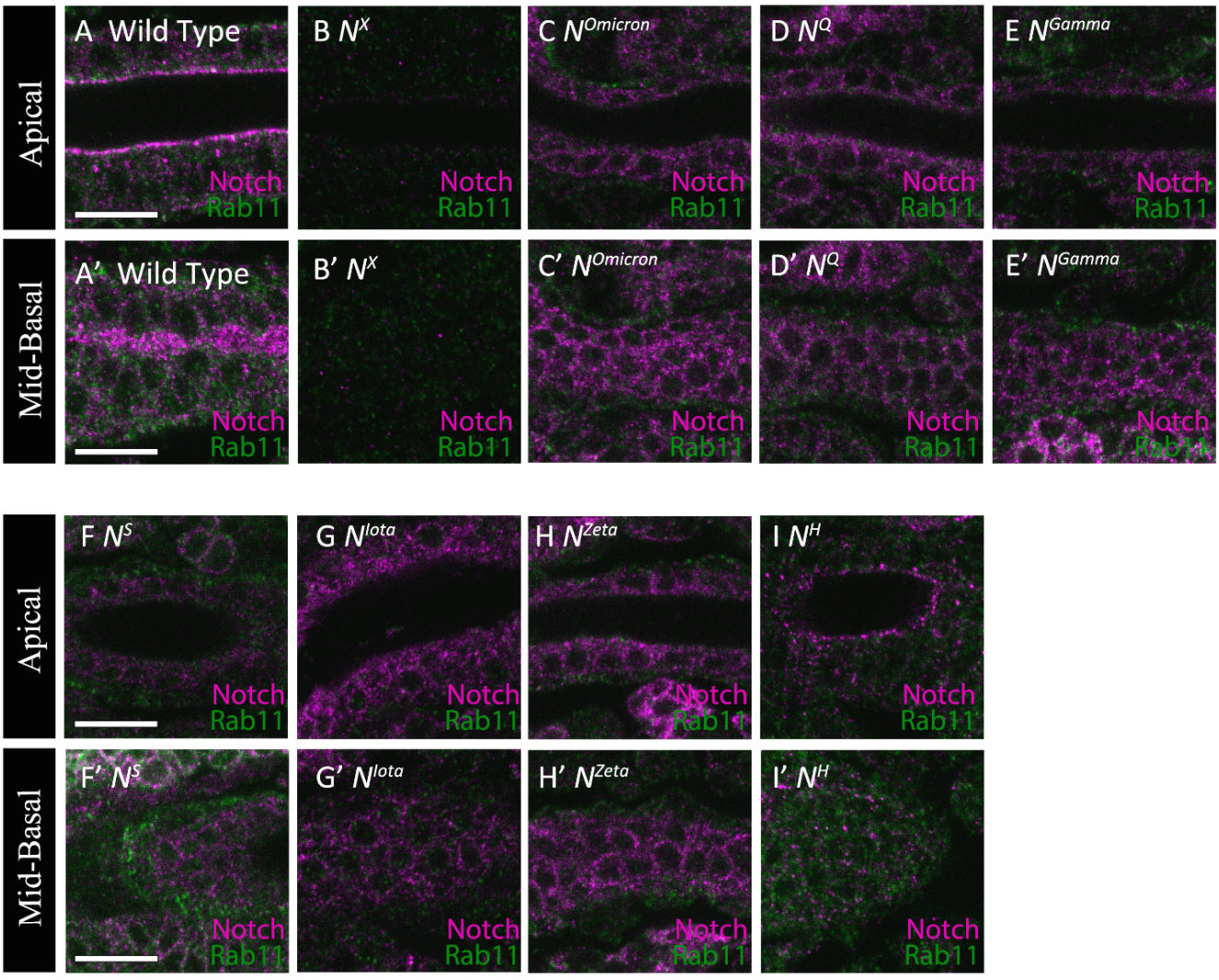

Figure 26. Class II and Class IV *Notch* mutants did not accumulate Notch in recycling endosomes

(A-I') Notch (magenta) and recycling endosomes (green), detected by anti-Notch and anti-Rab11 antibody staining, respectively, in hindgut epithelia in wild-type embryos (A and A') and hemizygotes of N^{X} (B and B'), $N^{omicron}$ (C and C'), N^{Q} (D and D'), N^{Gamma} (E and E'), N^{S} (F and F'), N^{Iota} (G and G'), N^{Zeta} (H and H'), and N^{H} (I and I'). Apical and mid-basal images (left side) correspond to the diagram of optical planes in Figure 17. Scale bars: 10 μm.

References

Adams, M. D., Celniker, S. E., Holt, R. A., Evans, C. A., Gocayne, J. D., Amanatides, P. G., Scherer, S. E., Li, P. W., Hoskins, R. A., Galle, R. F., George, R. A., Lewis, S. E., Richards, S., Ashburner, M., Henderson, S. N., Sutton, G. G., Wortman, J. R., Yandell, M. D., Zhang, Q., … Venter, J. C. (2000). The Genome Sequence of *Drosophila melanogaster*.*Science*, *287*(5461), 2185–2195. https://doi.org/10.1126/science.287.5461.2185

Andrawes, M.B.; Xu, X.; Liu, H.; Ficarro, S.B.; Marto, J.A.; Aster, J.C.; Blacklow, S.C. Intrinsic selectivity of Notch 1 for delta-like 4 over delta-like 1. *J. Biol. Chem.* **2013**, *288*, 25477–25489. https://doi.org/10.1074/jbc.M113.454850.

Arefin, B., Bahrampour, S., Monedero Cobeta, I., Curt, J. R., Stratmann, J., Yaghmaeian Salmani, B., Baumgardt, M., Benito-Sipos, J., & Thor, S. (2020). Development of the Drosophila melanogaster embryonic CNS. In *Patterning and Cell Type Specification in the Developing CNS and PNS* (pp. 617–642). Elsevier. https://doi.org/10.1016/B978-0-12-814405-3.00025-4

Arefin, B., Parvin, F., Bahrampour, S., Stadler, C. B., & Thor, S. (2019). Drosophila Neuroblast Selection Is Gated by *Notch*, Snail, SoxB, and EMT Gene

Interplay. *Cell Reports*, *29*(11), 3636-3651.e3. https://doi.org/10.1016/j.celrep.2019.11.038

Artavanis-Tsakonas, S., Rand, M. D., & Lake, R. J. (1999). *Notch* signaling: cell fate control and signal integration in development. *Science (New York, N.Y.)*, *284*(5415), 770–776. https://doi.org/10.1126/science.284.5415.770

Baron, M. (2003). An overview of the *Notch* signalling pathway. *Seminars in Cell & Developmental Biology*, *14*(2), 113–119. https://doi.org/10.1016/s1084-9521(02)00179-9

Baron, M. (2017). Combining genetic and biophysical approaches to probe the structure and function relationships of the *Notch* receptor. *Molecular Membrane Biology*, *34*(1–2), 33–49. https://doi.org/10.1080/09687688.2018.1503742

Becam, I., Fiuza, U.-M., Arias, A. M., & Milán, M. (2010). A Role of Receptor *Notch* in Ligand cis-Inhibition in Drosophila. *Current Biology*, *20*(6), 554–560. https://doi.org/10.1016/j.cub.2010.01.058

Berger, C., Renner, S., Lüer, K., & Technau, G. M. (2007). The commonly used marker ELAV is transiently expressed in neuroblasts and glial cells in the *Drosophila* embryonic CNS. *Developmental Dynamics*, *236*(12), 3562–3568. https://doi.org/10.1002/dvdy.21372

Bray, S. J. (2006). *Notch* signalling: a simple pathway becomes complex. *Nature Reviews Molecular Cell Biology*, *7*(9), 678–689. https://doi.org/10.1038/nrm2009

Bray, S. J. (2016). *Notch* signalling in context. *Nature Reviews Molecular Cell Biology*, *17*(11), 722–735. https://doi.org/10.1038/nrm.2016.94

Brennan, K., Tateson, R., Lewis, K., & Arias, A. M. (1997). A functional analysis of *Notch* mutations in Drosophila. *Genetics*, *147*(1), 177–188. https://doi.org/10.1093/genetics/147.1.177

Campbell, I. D., & Bork, P. (1993). Epidermal growth factor-like modules. *Current Opinion in Structural Biology*, *3*(3), 385–392. https://doi.org/10.1016/S0959-440X(05)80111-3

Cau, E., & Blader, P. (2009). *Notch* activity in the nervous system: to switch or not switch? *Neural Development*, *4*(1), 36. https://doi.org/10.1186/1749-8104-4-36

Chillakuri, C. R., Sheppard, D., Lea, S. M., & Handford, P. A. (2012). *Notch* receptor–ligand binding and activation: Insights from molecular studies. *Seminars in Cell & Developmental Biology*, *23*(4), 421–428. https://doi.org/10.1016/j.semcdb.2012.01.009

de Celis, J. F., & Bray, S. J. (2000). The Abruptex domain of *Notch* regulates negative interactions between *Notch*, its ligands and Fringe. *Development (Cambridge, England)*, *127*(6), 1291–1302.

Downing, A. K., Knott, V., Werner, J. M., Cardy, C. M., Campbell, I. D., & Handford, P. A. (1996). Solution Structure of a Pair of Calcium-Binding Epidermal Growth Factor-like Domains: Implications for the Marfan Syndrome and Other Genetic Disorders. *Cell*, *85*(4), 597–605. https://doi.org/10.1016/S0092-8674(00)81259-3

Fehon, R. G., Kooh, P. J., Rebay, I., Regan, C. L., Xu, T., Muskavitch, M. A. T., & Artavanis-Tsakonas, S. (1990). Molecular interactions between the protein products of the neurogenic loci *Notch* and *Delta*, two EGF-homologous genes in Drosophila. *Cell*, *61*(3), 523–534. https://doi.org/10.1016/0092-8674(90)90534-L

Feige, M. J., Braakman, I., & Hendershot, L. M. (2018). *CHAPTER 1.1. Disulfide Bonds in Protein Folding and Stability* (pp. 1–33). https://doi.org/10.1039/9781788013253-00001

Fuß, B., & Hoch, M. (2002). *Notch* Signaling Controls Cell Fate Specification along the Dorsoventral Axis of the Drosophila Gut. *Current Biology*, *12*(3), 171–179. https://doi.org/10.1016/S0960-9822(02)00653-X

Gazave, E., Lapébie, P., Richards, G. S., Brunet, F., Ereskovsky, A. v, Degnan, B. M., Borchiellini, C., Vervoort, M., & Renard, E. (2009). Origin and evolution of the *Notch* signalling pathway: an overview from eukaryotic genomes. *BMC Evolutionary Biology*, *9*, 249. https://doi.org/10.1186/1471-2148-9-249

Haelterman, N. A., Jiang, L., Li, Y., Bayat, V., Sandoval, H., Ugur, B., Tan, K. L., Zhang, K., Bei, D., Xiong, B., Charng, W.-L., Busby, T., Jawaid, A., David, G., Jaiswal, M., Venken, K. J. T., Yamamoto, S., Chen, R., & Bellen, H. J. (2014). Large-scale identification of chemically induced mutations in *Drosophila melanogaster*. *Genome Research*, *24*(10), 1707–1718. https://doi.org/10.1101/gr.174615.114

Haltom, A. R., & Jafar-Nejad, H. (2015). The multiple roles of epidermal growth factor repeat O-glycans in animal development. Glycobiology, 25(10), 1027–1042. https://doi.org/10.1093/glycob/cwv052

Hambleton, S., Valeyev, N. v., Muranyi, A., Knott, V., Werner, J. M., McMichael, A. J., Handford, P. A., & Downing, A. K. (2004). Structural and Functional Properties of the Human *Notch*-1 Ligand Binding Region. *Structure*, *12*(12), 2173–2183. https://doi.org/10.1016/j.str.2004.09.012

Iwaki, D. D., & Lengyel, J. A. (2002). A *Delta–Notch* signaling border regulated by Engrailed/Invected repression specifies boundary cells in the Drosophila hindgut.

Mechanisms of Development, *114*(1–2), 71–84. https://doi.org/10.1016/S0925-4773(02)00061-8

Kakuda, S. & Haltiwanger, R.S. (2017). Deciphering the fringe-mediated Notch code: Identification of activating and inhibiting sites allowing discrimination between ligands. *Dev. Cell*, *40*, 193–201. https://doi.org/10.1016/j.devcel.2016.12.013.

Kelley, M. R., Kidd, S., Deutsch, W. A., & Young, M. W. (1987). Mutations altering the structure of epidermal growth factor-like coding sequences at the Drosophila *Notch* locus. *Cell*, *51*(4), 539–548. https://doi.org/10.1016/0092-8674(87)90123-1

Kumichel, A., & Knust, E. (2014). Apical Localisation of Crumbs in the Boundary Cells of the Drosophila Hindgut Is Independent of Its Canonical Interaction Partner Stardust. *PLoS ONE*, *9*(4), e94038. https://doi.org/10.1371/journal.pone.0094038

Knott, V., Downing, K. A., Cardy, C. M., & Handford, P. (1996). Calcium Binding Properties of an Epidermal Growth Factor-like Domain Pair from Human Fibrillin-1. *Journal of Molecular Biology*, *255*(1), 22–27. https://doi.org/10.1006/jmbi.1996.0003

Lieber, T., Wesley, C. S., Alcamo, E., Hassel, B., Krane, J. F., Campos-Ortega, J. A., & Young, M. W. (1992). Single amino acid substitutions in EGF-like elements of

Notch and delta modify drosophila development and affect cell adhesion in vitro. *Neuron*, *9*(5), 847–859. https://doi.org/10.1016/0896-6273(92)90238-9

Lloyd, T. E., Atkinson, R., Wu, M. N., Zhou, Y., Pennetta, G., & Bellen, H. J. (2002). Hrs Regulates Endosome Membrane Invagination and Tyrosine Kinase Receptor Signaling in Drosophila. *Cell*, *108*(2), 261–269. https://doi.org/10.1016/S0092-8674(02)00611-6

Luca, V.C., Jude, K.M., Pierce, N.W., Nachury M., Fischer, S., Garcia, K.C. (2015). Structural basis for Notch1 engagement of Delta-like 4. *Science* **2015**, *347*, 847–853. https://doi.org/10.1126/science.1261093.

Luca, V.C., Kim, B.C., Ge, C., Kakuda, S., Wu, D., Roein-Peikar, M., Haltiwanger, R.S., Zhu, C., Ha, T., Garcia, K.C. (2017). Notch-Jagged complex structure implicates a catch bond in tuning ligand sensitivity. *Science*, *355*, 1320–1324. https://doi.org/10.1126/science.aaf9739.

Matsumoto, K., Ayukawa, T., Ishio, A., Sasamura, T., Yamakawa, T., & Matsuno, K. (2016). Dual Roles of O-Glucose Glycans Redundant with Monosaccharide O-Fucose on *Notch* in *Notch* Trafficking. *Journal of Biological Chemistry*, *291*(26), 13743–13752. https://doi.org/10.1074/jbc.M115.710483

Moore, R., & Alexandre, P. (2020). Delta-*Notch* Signaling: The Long and The Short of a Neuron's Influence on Progenitor Fates. *Journal of Developmental Biology*, *8*(2), 8. https://doi.org/10.3390/jdb8020008

Nagel, A. C., & Preiss, A. (1999). *Notch*splIs Deficient for Inductive Processes in the Eye, andE(spl)DEnhancessplitby Interfering with Proneural Activity. *Developmental Biology*, *208*(2), 406–415. https://doi.org/10.1006/dbio.1999.9203

O'Neill, E. M., Rebay, I., Tjian, R., & Rubin, G. M. (1994). The activities of two Ets-related transcription factors required for drosophila eye development are modulated by the Ras/MAPK pathway. *Cell*, *78*(1), 137–147. https://doi.org/10.1016/0092-8674(94)90580-0

O'Sullivan, N. C., Jahn, T. R., Reid, E., & O'Kane, C. J. (2012). Reticulon-like-1, the Drosophila orthologue of the Hereditary Spastic Paraplegia gene reticulon 2, is required for organization of endoplasmic reticulum and of distal motor axons. *Human Molecular Genetics*, *21*(15), 3356–3365. https://doi.org/10.1093/hmg/dds167

Oda, H., Uemura, T., Harada, Y., Iwai, Y., & Takeichi, M. (1994). A Drosophila Homolog of Cadherin Associated with Armadillo and Essential for Embryonic Cell-Cell Adhesion. *Developmental Biology*, *165*(2), 716–726. https://doi.org/10.1006/dbio.1994.1287

Okajima, T., Xu, A., & Irvine, K. D. (2003). Modulation of *Notch*-Ligand Binding by Protein O-Fucosyltransferase 1 and Fringe. *Journal of Biological Chemistry*, *278*(43), 42340–42345. https://doi.org/10.1074/jbc.M308687200

Okajima, T., Xu, A., Lei, L., & Irvine, K. D. (2005). Chaperone Activity of Protein *O* -Fucosyltransferase 1 Promotes *Notch* Receptor Folding. *Science*, *307*(5715), 1599–1603. https://doi.org/10.1126/science.1108995

Okajima, T., Reddy, B., Matsuda, T., & Irvine, K. D. (2008). Contributions of chaperone and glycosyltransferase activities of O-fucosyltransferase 1 to *Notch* signaling. *BMC Biology*, *6*(1), 1. https://doi.org/10.1186/1741-7007-6-1

Pandey, A., Harvey, B.M., Lopez, M.F., Ito, A., Haltiwanger, R.S., Jafar-Nejad, H. (2019). Glycosylation of specific Notch EGF repeats by O-Fut1 and fringe regulates notch signaling in drosophila. *Cell Rep.*, *29*, 2054–2066.e6. https://doi.org/10.1016/j.celrep.2019.10.027.

Pei, Z., & Baker, N. E. (2008). Competition between Delta and the Abruptex domain of *Notch*. *BMC Developmental Biology*, *8*(1), 4. https://doi.org/10.1186/1471-213X-8-4

Poellinger, L., & Lendahl, U. (2008). Modulating *Notch* signaling by pathway-intrinsic and pathway-extrinsic mechanisms. *Current Opinion in Genetics & Development*, *18*(5), 449–454. https://doi.org/10.1016/j.gde.2008.07.013

Rana, N. A., Nita-Lazar, A., Takeuchi, H., Kakuda, S., Luther, K. B., & Haltiwanger, R. S. (2011). O-Glucose Trisaccharide Is Present at High but Variable Stoichiometry at Multiple Sites on Mouse *Notch*1. *Journal of Biological Chemistry*, *286*(36), 31623–31637. https://doi.org/10.1074/jbc.M111.268243

Rand, M. D., Lindblom, A., Carlson, J., Villoutreix, B. O., & Stenflo, J. (2008). Calcium binding to tandem repeats of EGF-like modules. Expression and characterization of the EGF-like modules of human *Notch*-1 implicated in receptor-ligand interactions. *Protein Science*, *6*(10), 2059–2071. https://doi.org/10.1002/pro.5560061002

Rao,Z., Handford, P., Mayhew, M., Knott, V., Brownlee, G.G., Stuart, D., 1996, Epidermal growth factor-like domain from human factor IX,

DOI: 10.2210/pdb1EDM/pdb

Rebay, I., Fleming, R. J., Fehon, R. G., Cherbas, L., Cherbas, P., & Artavanis-Tsakonas, S. (1991). Specific EGF repeats of *Notch* mediate interactions with Delta and

serrate: Implications for *Notch* as a multifunctional receptor. *Cell*, *67*(4), 687–699. https://doi.org/10.1016/0092-8674(91)90064-6

Rhyu, M. S., Jan, L. Y., & Jan, Y. N. (1994). Asymmetric distribution of numb protein during division of the sensory organ precursor cell confers distinct fates to daughter cells. *Cell*, *76*(3), 477–491. https://doi.org/10.1016/0092-8674(94)90112-0

Roth, R. A., & Pierce, S. B. (1987). In vivo cross-linking of protein disulfide isomerase to immunoglobulins. *Biochemistry*, *26*(14), 4179–4182. https://doi.org/10.1021/bi00388a001

Sasaki, N., Sasamura, T., Ishikawa, H. O., Kanai, M., Ueda, R., Saigo, K., & Matsuno, K. (2007). Polarized exocytosis and transcytosis of *Notch* during its apical localization in Drosophila epithelial cells. *Genes to Cells*, *12*(1), 89–103. https://doi.org/10.1111/j.1365-2443.2007.01037.x

Sasamura, T., Sasaki, N., Miyashita, F., Nakao, S., Ishikawa, H. O., Ito, M., Kitagawa, M., Harigaya, K., Spana, E., Bilder, D., Perrimon, N., & Matsuno, K. (2003). *neurotic*, a novel maternal neurogenic gene, encodes an *O* -fucosyltransferase that is essential for *Notch*-Delta interactions. *Development*, *130*(20), 4785–4795. https://doi.org/10.1242/dev.00679

Schuster-Gossler, K., Cordes, R., Müller, J., Geffers, I., Delany-Heiken, P., Taft, M., Preller, M., & Gossler, A. (2016). Context-Dependent Sensitivity to Mutations Disrupting the Structural Integrity of Individual EGF Repeats in the Mouse *Notch* Ligand DLL1. *Genetics*, *202*(3), 1119–1133. https://doi.org/10.1534/genetics.115.184515

Schwanbeck, R., Martini, S., Bernoth, K., & Just, U. (2011). The *Notch* signaling pathway: Molecular basis of cell context dependency. *European Journal of Cell Biology*, *90*(6–7), 572–581. https://doi.org/10.1016/j.ejcb.2010.10.004

Schweisguth, F. (2004). Regulation of *Notch* Signaling Activity. *Current Biology*, *14*(3), R129–R138. https://doi.org/10.1016/j.cub.2004.01.023

Schweisguth, F. (2015). Asymmetric cell division in the *Drosophila* bristle lineage: from the polarization of sensory organ precursor cells to *Notch*-mediated binary fate decision. *Wiley Interdisciplinary Reviews: Developmental Biology*, *4*(3), 299–309. https://doi.org/10.1002/wdev.175

Siebel, C., & Lendahl, U. (2017). *Notch* Signaling in Development, Tissue Homeostasis, and Disease. *Physiological Reviews*, *97*(4), 1235–1294. https://doi.org/10.1152/physrev.00005.2017

Sjöqvist, M., & Andersson, E. R. (2019). Do as I say, Not(ch) as I do: Lateral control of cell fate. *Developmental Biology*, *447*(1), 58–70. https://doi.org/10.1016/j.ydbio.2017.09.032

Stanley, P., & Okajima, T. (2010). *Roles of Glycosylation in Notch Signaling* (pp. 131–164). https://doi.org/10.1016/S0070-2153(10)92004-8

Suzuki, M., Hara, Y., Takagi, C., Yamamoto, T. S., & Ueno, N. (2010). MID1 and MID2 are required for Xenopus neural tube closure through the regulation of microtubule organization. *Development (Cambridge, England)*, *137*(14), 2329–2339. https://doi.org/10.1242/dev.048769

Suckling, R., Johnson, S., Lea, S.M., 2020, Structure of *Drosophila Notch* EGF Domains 11-13, **DOI:** 10.2210/pdb7ALJ/pdb

Takashima, S., Yoshimori, H., Yamasaki, N., Matsuno, K., & Murakami, R. (2002). Cell-fate choice and boundary formation by combined action of *Notch* and engrailed in the Drosophila hindgut. *Development Genes and Evolution*, *212*(11), 534–541. https://doi.org/10.1007/s00427-002-0262-z

Tanaka, T., & Nakamura, A. (2008). The endocytic pathway acts downstream of Oskar in *Drosophila* germ plasm assembly. *Development*, *135*(6), 1107–1117. https://doi.org/10.1242/dev.017293

Tepass, U., & Knust, E. (1993). crumbs and stardust Act in a Genetic Pathway That Controls the Organization of Epithelia in Drosophila melanogaster. *Developmental Biology*, *159*(1), 311–326. https://doi.org/10.1006/dbio.1993.1243

Tombling, B. J., Wang, C. K., & Craik, D. J. (2020). EGF-like and Other Disulfide-rich Microdomains as Therapeutic Scaffolds. *Angewandte Chemie International Edition*, *59*(28), 11218–11232. https://doi.org/10.1002/anie.201913809

Wouters, M. A., Rigoutsos, I., Chu, C. K., Feng, L. L., Sparrow, D. B., & Dunwoodie, S. L. (2005). Evolution of distinct EGF domains with specific functions. Protein Science, 14(4), 1091–1103. https://doi.org/10.1110/ps.041207005

Yamakawa, T., Yamada, K., Sasamura, T., Nakazawa, N., Kanai, M., Suzuki, E., Fortini, M. E., & Matsuno, K. (2012). Deficient *Notch* signaling associated with neurogenic *pecanex* is compensated for by the unfolded protein response in *Drosophila*. *Development*, *139*(3), 558–567. https://doi.org/10.1242/dev.073858

Yamamoto, S., Charng, W.-L., & Bellen, H. J. (2010). *Endocytosis and Intracellular Trafficking of Notch and Its Ligands* (pp. 165–200). https://doi.org/10.1016/S0070-2153(10)92005-X

Yamamoto, S., Charng, W.-L., Rana, N. A., Kakuda, S., Jaiswal, M., Bayat, V., Xiong, B., Zhang, K., Sandoval, H., David, G., Wang, H., Haltiwanger, R. S., & Bellen, H. J. (2012). A Mutation in EGF Repeat-8 of *Notch* Discriminates Between Serrate/Jagged and Delta Family Ligands. *Science*, *338*(6111), 1229–1232. https://doi.org/10.1126/science.1228745

Yamamoto, S., Jaiswal, M., Charng, W.-L., Gambin, T., Karaca, E., Mirzaa, G., Wiszniewski, W., Sandoval, H., Haelterman, N. A., Xiong, B., Zhang, K., Bayat, V., David, G., Li, T., Chen, K., Gala, U., Harel, T., Pehlivan, D., Penney, S., … Bellen, H. J. (2014). A Drosophila Genetic Resource of Mutants to Study Mechanisms Underlying Human Genetic Diseases. *Cell*, *159*(1), 200–214. https://doi.org/10.1016/j.cell.2014.09.002

Yamamoto, S. (2020). Making sense out of missense mutations: Mechanistic dissection of *Notch* receptors through structure-function studies in *Drosophila*. *Development, Growth & Differentiation*, *62*(1), 15–34. https://doi.org/10.1111/dgd.12640

Acknowledgement

I would like to send my sincere gratitude toward Prof. Kenji Matsuno for his guidance and opportunity which is given to me throughout this doctoral period

I would like to also express my appreciations toward the committee members, Prof. Naotada Ishihara, Prof. Hiroki Oda and Prof. Motoo Kitagawa for their thoughtful inputs and also advices for me during this doctoral period

Special thanks also given to our collaborator, Dr. Shinya Yamamoto for his gifts of *Notch* mutants, therefore I can conduct this experiment, and for the thoughtful discussions following this research

My deep appreciation given to the members of the Matsuno Lab, Osaka University for the continuous supports, therefore I can finish the experiment. Especially for the assistant professors Dr. Takeshi Sasamura, Dr. Mikiko Inaki and Dr. Tomoko Yamakawa for the guidances and advices during my time in the laboratory

I want to thank Bloomington *Drosophila* stock center, Kyoto stock center, Developmental studies of hybridoma bank and Prof. Hugo Bellen Lab., for the fly stocks and the antibodies which used in this research

Finally, I also want to thank God for the opportunity given to me, my families, my friends and everyone whom always motivate and support me during the time, therefore I could finish this study

Hilman Nurmahdi is supported by Osaka University Next Generation Fellowship